Cellulose Nanofiber and Dye from Oil Palm Tree

Kamthorn Intharapichai
Kyoto Institute of Technology

2019

Contents

Chapter 1

General Introduction

1.1.   Background of the work

Petroleum is a limited fossil resource; therefore, the human race will eventually need to become less dependent on it. Additionally, plastics produced from petroleum significantly increase the amount of carbon dioxide released into the atmosphere when they are incinerated after use. Furthermore, non-degradable plastics damage the ecosystem because they accumulate in the natural environment. In particular, there is a concern that microplastics in the sea will eventually reach humans via the food chain as a result of plankton getting into the microplastics and fish eating the plankton.

Some plants contain substances used in herbal medicine and natural dyes; they are difficult to produce using chemical synthesis. In particular, natural dye is currently popular owing to consumers' increased preference for organic products. Plants are a type of biomass that exist in the Earth in large quantities and are a renewable resource, taking carbon dioxide in from the atmosphere using sunlight. Therefore, products made from plants do not increase atmospheric carbon dioxide. Plants have long been used as structural materials; they have supported our clothing, food, and housing and are compatible with the environment.

Despite these advantages, plants are still difficult to use in industrial materials because of their instability and processing challenges. In Southeast Asia, many plants come from plantations, such as oil palms, sugar cane, and rubber trees. These natural resources are expected to be a driving force for future economic development.

Chapter 1

1.2.   Oil palm tree

The annual production of plant oils is increasing year by year. In particular, palm oil has the highest level of production and is growing at a high rate [1] (Fig. 1.1). Oil palm from West Africa is classified as *Elaeis guineensis*, and oil palm from Latin America is classified as *Elaeis oleifera*. *Elaeis guineensis* was introduced into Sumatra and the Malay Peninsula in the early 1900s, and vast plantations are now underway [2]. Warm and rainy climate conditions are required for oil palm cultivation, and the north–south latitude range of 10 degrees is considered suitable for cultivation. Oil palm is different from the coconut palm, which is generally imaged, and has a lower height, of 15–20 m.

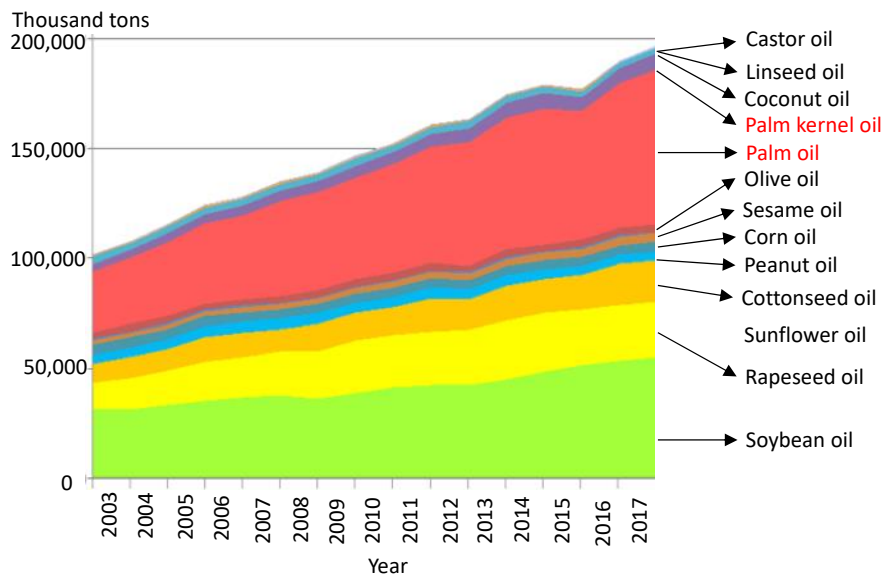**Fig. 1.1.**   Plant oil production in the world.

Palm oil is obtained from the pulp of the palm fruit, and palm kernel oil is obtained from the fruit's central seed [3]. When oil palm is cultivated, 80% is used for foods and the remaining is used in cosmetics, soap, paint, and industrial lubricant. In recent years, the industrial production of biodiesel fuel from exploited oil has become

2

Chapter 1

popular. Palm oil can be harvested in large quantities throughout the year, and its production is increasing worldwide.

Malaysia and Indonesia are the first and second largest producers of palm oil, respectively, producing 85% of the world's palm oil between them. The two countries are rich in natural habitat; however, oil palm tree plantations have destroyed this habitat, and endangered species, such as the orangutan, is under greater threat. Although palm oil cultivation is very popular in Thailand, after Malaysia and Indonesia, its forest administration is undertaken by the Ministry of Natural Resources and Environment, which promotes forest conservation and protection [4].

1.3. Cellulose nanofiber

Besides biodegradability and renewability, the production of nano-dimensional cellulosic fibers adds promising properties, such as high mechanical characteristics and low density [5,6]. Although cellulose microfibrils and bundles of cellulose microfibrils cannot be measured directly, the elastic modulus and tensile strength of crystalline cellulose microfibrils are 140 GPa and 2–3 GPa, respectively, estimated from kraft pulping, which is the aggregation of cellulose microfibrils [7]. The elastic modulus is stable from −200°C to 200°C [8], and the linear thermal expansion coefficient of the cellulose material in the fiber direction is 0.17 ppm/K [9]. This value is comparable to that of quartz glass, and the CNF sheets' thermal conductivity is comparable to that of glass [10].

CNF is divided into three types: single CNF (cellulose microfibril) is the most basic structure, with a width of 4 nm; cellulose microfibril is the basic unit of the cell wall, which is the bundle of several single celluloses, with a width of 10–20 nm; and
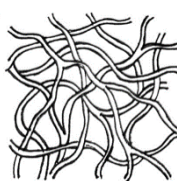
Chapter 1

microfibrillated cellulose (MFC) is a bundle of several dozen or hundreds of cellulose microfibrils that form a spider web network [11]. In addition to these three types, the cellulose nanocrystals (CNC) are usually isolated from cellulose fibers through acid hydrolysis [12–14]. The particles are 100% cellulose and highly crystalline, varying between 54% and 88% crystalline zones [15].

CNF can be produced from almost any plant, but generally wood pulp is used as the raw material [16]. Several methods for producing CNF have been developed. Oxidation via the 2,2,6,6-tetram-ethyl-1-piperidinyloxy radical (TEMPO) is applied to wood celluloses in water, and almost all glucosyl units exposed to crystalline cellulose microfibrils are selectively oxidized to sodium glucuronosyl units. The TEMPO-oxidized cellulose obtained in this way has the same fibrous morphologies as original wood cellulose [17,18]. Grinding is the fibrillation of wood pulp fibers into nanofibers [19]. An aqueous counter collision method for cellulose that can be downsized into nano-objects uses only a high-speed water jet as the medium, without chemical modification of molecules, including depolymerization [20]. Enzymatic hydrolysis of microcrystalline cellulose involves two crystalline allomorphs of cellulose [21]. Another type of nanocellulose is bacterial nanocellulose (BNC), which is synthesized from glucose with a bottom-up method by a family of bacteria, referred to as *Gluconoacetobacter xylinius* [22]. Due to its light weight and its strength, CNF is used to reinforce fiber in plastics. Automobile parts require not only high strength but also light weight to improve fuel economy. Adding CNF to cosmetics makes them cleaner. Adding CNF to food changes the texture, even creating non-melting ice cream. The film's high gas barrier is an important property since it can be used for high-performance electronic devices [23].

Chapter 1

Table 1.1. Types, structures, and methods of cellulose nanofiber.

	Width (nm)	Structure	Image	Method
Single cellulose nanofiber	4	Single fiber		TEMPO Bacteria
Cellulose microfibril	10–20	Bundle of single fiber		Grinder
Microfibrillated cellulose	5–60	Bundle and web network of cellulose microfibrils		High pressure homogenizer
Cellulose nanocrystal	5–70	Rod (Length: 100–250 nm)		Hydrolysis of cellulose fibers

1.4. Natural Dyes

Natural dyes have been used for many years. For example, flax fibers found in the Dzudzuana caves at the foothills of the Caucasus, Georgia, are estimated to have been dyed 26 to 32 thousand years ago [24]. Natural dyes are produced and used today, whereas synthetic dyes have replaced the mainstream dyes since they were invented [25].

The pigment molecules and their precursors, which are synthesized in the bodies of plants and animals, play a variety of roles. Chlorophyll for photosynthesis, melanin for protective functions, and retinols for eyesight are well known. Some pigments are mainly used as textile dyes. The typical types of natural dyes are indole derivatives, carotenoids,

diarylheptanoids, isoquinoline alkaloids, anthocyanins, chalcones, flavonoids, catechol tannins, pyrogallol tannins, ellagic acids, caffeic acid derivatives, naphthoquinone derivatives, neoflavonoids, and anthraquinone derivatives. The source of the natural dyes and the resulting colors of the fibers dyed by them are summarized in technical articles [26,27].

One of the characteristics of the colorants obtained from plants and animals, when they are used as a single dye, is that they are mixtures of pigments and other components. That is, while a synthetic dye is sometimes used as a single component of the dye, without color matching, natural dyes always contain plural colorants when not completely refined. This influences the dyeing results and resulting color. Since natural dye components are not uniform, dyeing under the same conditions will produce inconsistent colors. Purifying natural dyes is not easy because they are active and change chemically during the purification process. Moreover, such purification is unnecessary in the production of dyes in factories. This means that color control is not easy when using natural dyes.

Mordanting is often required to obtain deep colors and achieve sufficient color fastness when using natural dyes, except for indigo dyeing and dyeing with cationic dye molecules. This increases the number of steps in the dyeing process. To obtain sufficient dyeability, it is necessary to repeat the dyeing process with natural dyes.

However, some natural dyes and dye precursors are chemically active and exhibit intrinsic characteristics [28,29,30]. For example, flavonoids exist in plants such as glycosides. Their aglycones have phenolic hydroxyl groups and exhibit reducing properties [26].

Dyeing and functional finishing with natural dyes that take advantage of their unique characteristics is important and interesting work.

Chapter 1

1.5.   Purpose of the Study

In this study, oil palm trees are highlighted, among many other plants, because of the widespread plantations that provide useful ingredients. In particular, the purpose of the study is to produce CNF and dyes from oil palm trees.

CNF will be generated from three types of oil palm waste, i.e., palm pressed fiber, empty fruit bunches, and palm kernel shells, as well as from oil palm tree trunks. Their morphological, thermal, and mechanical properties will then be compared.

Another purpose of the study is to examine the dyeability of the extracts from each part of the silk fabric. Then the author will investigate the dependence of the dyeability of silk fabrics on the extract concentration in the dye solution, the dyeing time, and the dyeing temperature. The author will also evaluate the dyeability of natural fiber extracts, such as wool, cotton, and ramie, and of synthetic fibers, such as acrylic, polyester, and nylon.

Chapter 1

References

[1]   Oil world annual-Global analysis of all major oilseeds, oils and oilmeals supply, demand and price outlook-, ISTA Mielke

[2]   Blaizat, P. and Cuvier, P.; A new source of carotene: palm fiber oil from *Elaeis guineensis*, *Journal of the American Oil Chemists' Society*, 30, 586–587 (1953)

[3]   Corley, R. H. V. and Tinker, P. B.; The origin and development of the oil palm industry, the classification and morphology of the oil palm (Chapter 1 and 2), In The oil palm, Fourth edition, Blackwell Science, Oxford, 1–52 (2007)

[4]   Status of tropical forest management, International tropical timber organization, p.p. 242–252 (2011)

[5]   De Mesquita, J. P., Donnici, C. L., and Pereira, F. V.; Biobased nanocomposites from layer-by-layer assembly of cellulose nanowhiskers with chitosan, *Biomacromolecules*, 11, 473–480 (2010)

[6]   Yano, H. and Nakahara, S.; Bio-composites produced from plant microfiber bundles with a nanometer unit web-like network, *Journal of Material Science*, 39, 1635–1638 (2004)

[7]   Sakurada, I., Nukushina, Y., and Ito, T.; Experimental determination of the elastic modulus of crystalline regions in oriented polymers, *Journal of Polymer Science*, 57, 651–660, (1962)

[8]   Nishino, T., Kotera, M., and Kimoto, M.; 2nd Int'l Cellulose Conf. 2007, 125, (2007)

[9]   Nishino, T., Matsuda, I., and Hirao, K.; The use of cellulose nanofillers in obtaining polymer nanocomposites: Properties, Processing, and Applications, *Macromolecules*, 37, 7683–7687 (2004)

Chapter 1

[10] Shimazaki, Y., Miyazaki, Y., Takezawa, Y., Nogi, M., Abe, K., Ifuku, S., and Yano, H.; Excellent thermal conductivity of transparent cellulose nanofiber/epoxy resin nanocomposites, *Biomacromolecules*, 8, 2976–2978 (2007)

[11] Yano, H.; Production of cellulose nanofibers and their applications, *Rubber science and technology*, *Japan*, 85, 376–381 (2012)

[12] Tanpichai, S., Quero, F., Nogi, M., Yano, H., Young, R. J., Lindström, T., Sampson, W. W., and Eichhorn, S. J.; Effective young's modulus of bacterial and microfibrillated cellulose fibrils in fibrous networks, *Biomacromolecules*, 13, 1340–1349 (2012)

[13] Bhatnagar, A., and Sain, M.; Processing of cellulose nanofiber reinforced composites, *Journal of Reinforced Plastic Composite*, 24, 1259–1268 (2005)

[14] Cranston, E. D. and Gray, D. G.; Morphological and optical characterization of polyelectrolyte multilayers incorporating nanocrystalline cellulose, *Biomacromolecules*, 7, 2522–2530 (2006)

[15] Moon, R. J., Martini, A., Nairn, J., Simonsen, J., and Youngblood, J.; Cellulose nano-materials review: Structure, properties and nanocomposites, *Chemical Society Review*, 40, 3941–3994 (2011)

[16] Yano, H.; Cellulose nanofibers -Future materials based on sustainable resource in Japan-, Sustainable humanosphere; *Bulletin of Research Institute for Sustainable Humanosphere Kyoto University*, 14, 1–7 (2018)

[17] Isogai, A.; Composite materials of TEMPO-oxidized cellulose single nanofiber, *Rubber science and technology*, *Japan*, 85, 388–393 (2012)

Chapter 1

[18] Saito, T. and Isogai, A.; TEMPO-mediated oxidation of native cellulose, The effect of oxidation conditions on chemical and crystal structures of the water-insoluble fractions, *Biomacromolecules*, 5, 1983–1989 (2004)

[19] Iwamoto, S., Nakagaito, A. N., Yano, H., and Nogi, M.; Optically transparent composites reinforced with plant fiber-based nanofibers, *Applied Physics A: Materials Science and Processing*, 81, 1109–1112 (2005)

[20] Kondo, T.; Preparation of single cellulose nanofibers dispersed in water using aqueous counter collision method, *Journal of the Society of Rubber science and technology*, *Japan*, 85, 400–405 (2012)

[21] Hayashi, N., Kondo, T., and Ishihara, M.; Enzymatically produced nano-ordered short elements containing cellulose I_β crystalline domains, *Carbohydrate Polymers*, 61, 191–197 (2005)

[22] Klemm, D., Kramer, F., Moritz, S., Lindström, T., Ankerfors, M., Gray, D., and Dorris, A.; Nanocelluloses: A new family of nature-based materials, *Angewandte Chemi International Edition*, 50, 5438–5466 (2011)

[23] Yano, H.; Production of cellulose nanofibers and their applications, *Journal of the Society of Rubber Science and Technology*, *Japan*, 85, 376–381 (2012)

[24] Kvavadze, E., Bar-Yosef, O., Belfer-Cohen, A., Boaretto, E., Jakeli, N., Matskevich, Z., and Meshveliani, T.; 30,000-year-old wild flax fibers, *Science*, 325, 1359 (2009)

[25] Hunger, K. ed.; *Industrial dyes*: *chemistry, properties, applications*, Chap. 1, Chap. 2, Chap. 4, Wiley-VCH (2003)

[26] Bechtold, T. and Mussak, R. eds.; Handbook of natural colorants, p.p. 40, p.p. 66, p.p. 136, p.p. 261, Wiley (2009)

[27] Vankar, P. S.; *Natural dyes for textiles*, Chap. 4, Elsevier (2017)

[28] Yasunaga, H., Takahashi, A., Ito, K., Ueda, M., and Urakawa, H.; Hair dyeing by using catechinone obtained from (+)-catechin, *Journal of Cosmetics, Dermatological Sciences and Applications*, 2, 158–163 (2012)

[29] Matsubara, T., Wataoka, I., Urakawa, H., and Yasunaga, H.; Effect of reaction pH and $CuSO_4$ addition on the formation of catechinone due to oxidation of (+)-catechin, *International Journal of Cosmetic Science*, 35, 362–367 (2013)

[30] Maaza, M.; Novel plant bioresources (Gurib-Fakim, A. ed.), Chapter 35, 479, Wiley-Blackwell (2014)

[31] Giusti, M. M. and Wallace, T. C.; Handbook of natural colorants (Bechtold, T. and Mussak, R. eds.), p.p. 264–266, Wiley (2009)

Chapter 2

Comparison of Cellulose Nanofiber Properties Produced from Different Parts of the Oil Palm Tree

2.1. Introduction

The oil palm tree (*Elaeis guineensis*) is one of the most important commercial oil crops. During the last century, large-scale oil palm plantations were developed in southeastern Asian countries. These trees can be harvested throughout the year, but they also pose serious problems concerning waste handling [1,2]. Palm pressed fiber (PPF), empty fruit bunch (EFB), and palm kernel shell (PKS) are three important types of waste materials left in the palm-oil mill [3]. This biomass has limited uses, such as the production of an organic fertilizer or combustion to generate electricity [1,4]. Moreover, when left on the floor, these waste materials create significant environmental problems [1]. One of the approaches to solve this problem is the development of new applications for oil palm residues.

Recently, the production of cellulose nanofibers (CNF) and their applications in composite materials has gained significant interest due to their high Young's modulus, high strength, low coefficient of thermal expansion, low weight, biodegradability, and renewability [5,6]. The expected applications of CNF include structural materials for automobiles, flexible electronic substrates, packaging for food and medical supplies with high oxygen-barrier properties and gas separation membranes [7,8]. The production of CNF should be an effective utilization of oil palm residues.

Cellulose is the major constituent of plant cell walls. Many researchers have studied the extraction of cellulose nanofibers from biomass materials [9–16]. Some efforts have been made to isolate and characterize CNF from EFB [17–19], and research on the isolation of cellulose nanocrystals from PPF and tree trunks using acid hydrolysis has been reported [20,21].

Chapter 2

These studies mainly focused on the method for the isolation of CNF or nanocrystals from oil palm samples, and succeeded obtaining them by using different techniques. However, no research has been reported on CNF isolated from the PPF and PKS, nor on a direct comparison of the CNF properties obtained from different parts of oil palm tree. The degree of polymerization, structure, morphology, and surface properties of the resulting CNF can be very different depending on the raw materials [5,22,23]. PPF, EFB, and PKS have different cell wall structures and chemical components from each other [24], because they come from different parts of the tree. It could be that the performances of CNF differ depending on which part of the plant is used as a raw material. Here, the author produced CNF from three types of oil palm wastes, PPF, EFB, and PKS, as well as the oil palm tree trunk, to compare their morphological, thermal and mechanical properties.

2.2.   Materials and Methods

2.2.1.   Materials

Oil palm PPF, EFB, PKS, and trunk were obtained from Suksomboon Palm Oil Co., Ltd (Chonburi, Thailand) (Fig. 2.1). All samples were ground and dried under reduced pressure at ambient temperature. The α-cellulose content was measured following the method of [25]. The holocellulose (cellulose and hemicellulose) content was determined according to the method by [26]. Hemicellulose content was obtained from the difference in the amount of holocellulose and α-cellulose. The lignin content of the samples was determined based on the amount of sulfuric acid-insoluble Klason lignin described by [27]. The composition ratio varied with the samples. The PPF contained the lowest hemicellulose, and the PKS contained the highest lignin (Table 2.1). These results were in good agreement with previous reports [24]. However, it must be noted that Klason lignin also contains proteins when applied to plant-based food products [28].

Chapter 2
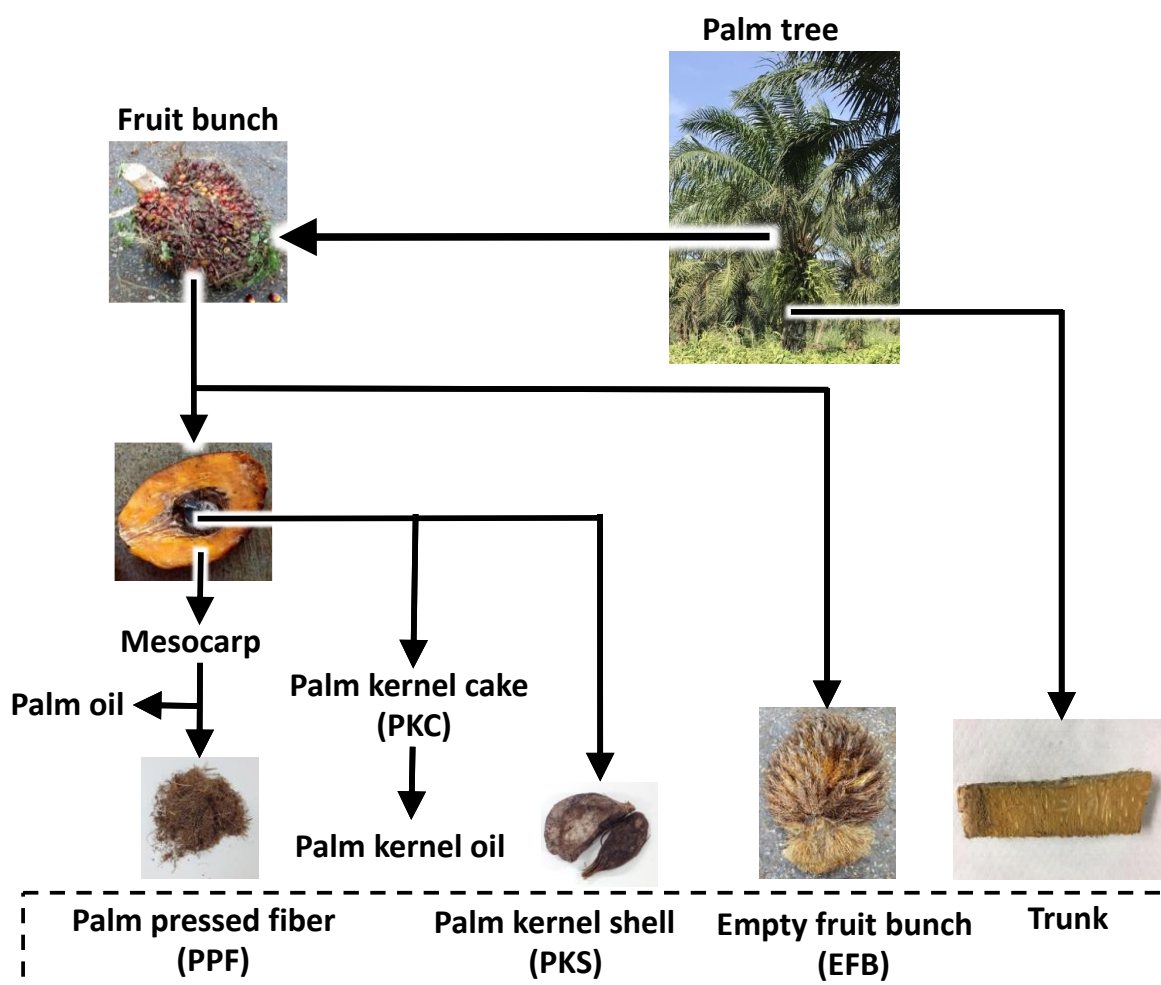
Fig. 2.1.   Raw materials for this study. The mesocarp is the fleshy middle layer of the pericarp

of a fruit and pressed to obtain palm oil remaining palm pressed fiber. The pulp left

after oil is rendered from the kernel is formed into palm kernel cake.

Table 2.1.   Chemical composition of raw materials.

Sample	Cellulose (wt%)	Hemicellulose (wt%)	Lignin (wt%)
Palm pressed fiber	39.7	15.0	31.4
Empty fruit bunch	38.7	31.0	25.6
Palm kernel shell	25.4	27.5	38.7
Trunk	36.7	39.2	24.5

Chapter 2

2.2.2. Purification of cellulose fibers

The reagents used in this study were supplied by WAKO Pure Chemical Industries Ltd (Osaka, Japan). Sample extracts were prepared with a 1:2 (v/v) methanol/toluene solution using a Soxhlet apparatus over 12 h. Samples were cyclically treated in an acidified sodium chlorite (NaClO$_2$) solution at 70°C for 1 h, until the product became white as a result of lignin leaching [27]. To leach hemicelluloses, samples were treated in a 5 wt% potassium hydroxide (KOH) solution overnight at ambient temperature, and then at 80°C for 2 h. This was repeated until the α-cellulose content was over 85%. After the chemical treatments, the samples were filtered and rinsed with distilled water until the residues were neutral.

2.2.3. Preparation of cellulose nanofiber sheets

A slurry of 1 wt% of purified cellulose was passed once through a grinder (MKCA6-3, Masuko Sangyo Co., Saitama, Japan) at 1500 rpm with the grinding stones (NKGC6-120, Masuko) pressed closely together. CNF sheets, 90 mm in diameter, were obtained from 120 g of fibrillated slurry with a fiber content of 0.5 wt% by filtration.

2.2.4. Characterization

2.2.4.1. Fourier-transform infrared spectroscopy

Raw materials and purified cellulose were analyzed using attenuated total reflection Fourier transform infrared (ATR-FTIR) spectroscopy (Spectrum One, PerkinElmer, Inc., USA) to examine the changes in functional groups induced by purification of cellulose and to compare them among samples. Spectra was collected in the range of 4000–650 cm^{-1}, at a resolution of 4 cm^{-1}.

2.2.4.2. Atomic force microscopy observation

The surfaces of the CNF sheets were imaged by AFM (AFM5100N, Hitachi High-Tech Science Co., Tokyo Japan). The specimens were scanned under dynamic force mode probes with a tip radius of 7 nm. The length of the cantilever was 200 µm, the spring constant

was 9 N/m, and the resonant frequency was 150 kHz. Real-time scanning was performed with scan rates of 0.5–1.0 Hz and scan angle 0°. Images were obtained in the phase mode.

2.2.4.3. X-ray diffraction analysis

X-ray diffraction (XRD) patterns of the CNF sheets were recorded. Cu Kα radiation was generated by a RINT-2500 (Rigaku Co., Tokyo Japan) diffractometer, operated at 40 kV and 20 mA, with a scan speed of 0.5°/min, sampling step angle of 0.02°, and scan range $2\theta =$ 5°–40°. The diffractometer was operated in reflection mode, and cellulose nanofiber sheets were irradiated in the direction perpendicular to the surface.

Crystallinity (CrI) was calculated using Segal's method via Eq. (2.1) [29].

$$\text{CrI} = \frac{I_c - I_a}{I_c} \qquad\qquad (2.1)$$

In this equation, I_c means the maximum intensity at 2θ (between 22° and 23°) for cellulose I, and I_a refers to the minimum intensity at 2θ for cellulose I.

The crystallite size D was calculated using Scherrer's Eq. (2.2) [30].

$$D = \frac{\lambda}{\beta \cos\theta} \qquad\qquad (2.2)$$

where $\lambda = 1.5418$ Å, β: corrected integral width, θ: Bragg angle for the 200 reflection.

2.2.4.4. Thermogravimetric analysis

Thermogravimetric analysis (TGA) of the CNF sheets was conducted using a thermogravimetric analyzer (STA7200 RV, Hitachi High-Tech Science Co., Tokyo, Japan) with a rate of 10°C/min from ambient temperature to 600°C after heating at 110°C for 20 min to dehydrate the samples. The analyses were performed in a nitrogen atmosphere with a 60 ml/min flow rate.

2.2.4.5. Tensile test

A rectangular-shaped specimen (5 × 40 mm) of each CNF sheet was formed using a cutter, and the specimen was completely dried in vacuo at 40°C for over 12 h before use. Tensile moduli of fibrillated-fiber sheets were evaluated using Universal materials testing machine (EZ-

Chapter 2

SX, Shimadzu Co., Kyoto, Japan) for samples 20 mm long and 3 mm wide at a crosshead speed of 1 mm/min. The average values ± standard deviations of Young's modulus, tensile strength and strain at break were evaluated using five independent specimens.

2.3. Results and Discussion

2.3.1. Fourier transform infrared spectra

The FTIR spectra of raw materials and purified cellulose are shown in Fig. 2.2. As expected from the chemical compositions of the raw materials (Table 2.1), the spectra of raw materials varied with each sample (Fig. 2.2-a). The absorption bands at 1425, 1501, and 1610 cm^{-1}, associated with the aromatic rings in lignin [31,32], occurred in all samples and were especially strong in the PKS. The absorption band at 1730 cm^{-1}, associated with hemicellulose, also appeared in all spectra (Fig. 2.2-a). In addition, the absorption derived from protein at 1233 cm^{-1}, amide III [33], was seen in all samples.   A certain absorption appeared at 2000–2260 cm^{-1}, which can be associated with Si-H from silica [34]. It has been reported that silica bodies were observed on the surface of the EFB fiber [4]. In this study, the existence of silica bodies on other oil palm residue fibers was suggested.

After the purification, the absorption peaks corresponding to lignin, hemicelluloses, protein, and silica were diminished in their intensity in all samples, confirming the removal of these components (Fig. 2.2-b). The absorption band at 897–1160 associated with cellulose [4,33] was present in all spectra (Fig. 2.2-b). It can be seen that the purification of cellulose by acidified sodium chlorite treatment and alkaline treatment succeeded in all samples.
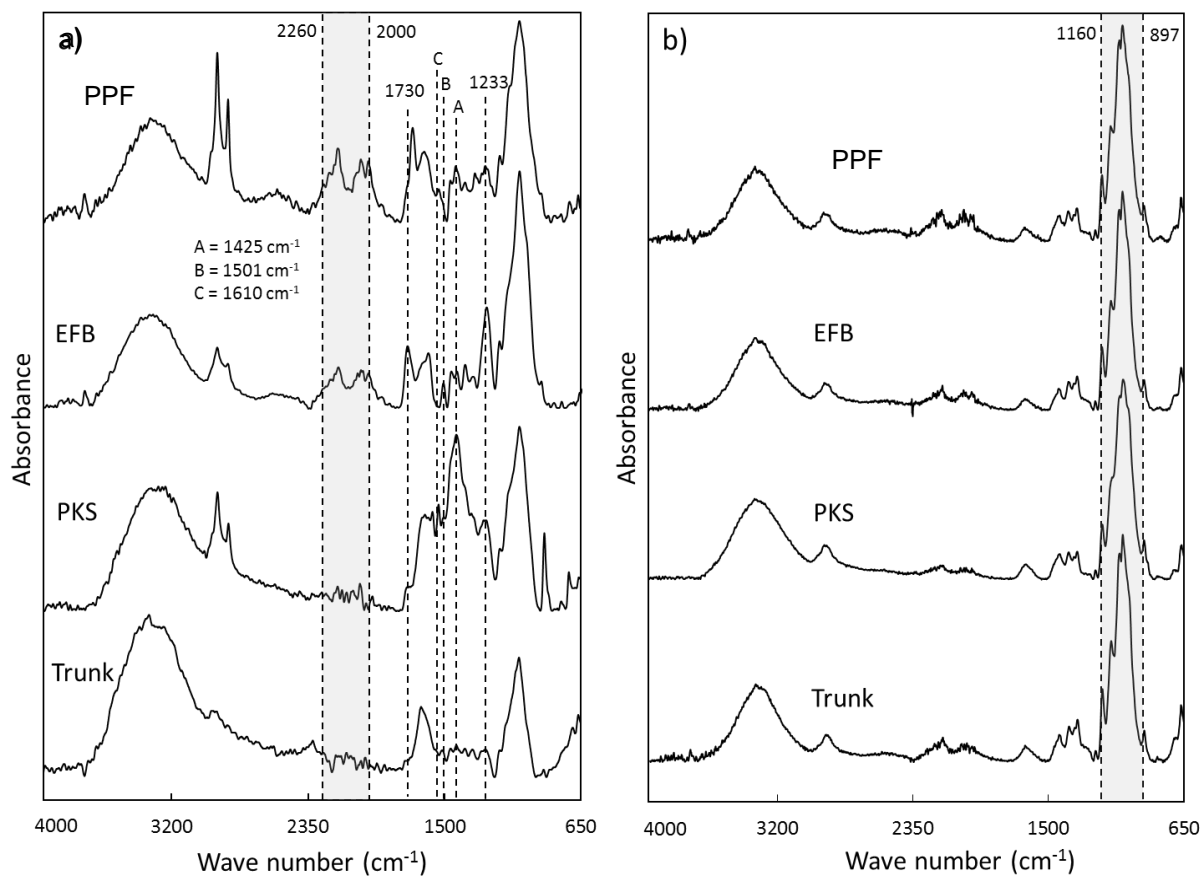
Fig. 2.2. Fourier-transform infrared spectra of raw materials (a), and purified cellulose (b).

2.3.2. Morphological observation of sheets

The CNF sheets were prepared using the same concentrations of CNF dispersion. The thicknesses of the CNF sheets from the PPF, EFB, PKS, and trunk were 158, 155, 147, and 152 μm, respectively. The CNF sheets from the EFB, PKS, and trunk appeared translucent, and only the PPF sheet was not transparent. (Fig. 2.3). If the CNF are densely packed, and the interstices between the fibers are small enough to avoid light scattering, the cellulosic material becomes transparent [35]. It was suggested that the CNF from the PPF contains larger aggregations of fibers which caused light scattering. Another possible reason was browning by Maillard reaction. This reaction is known as non-enzymatic browning and is a naturally occurring

reaction involving condensation of a reducing sugar or polysaccharide with protein or peptide, by linking the reducing end carbonyl groups in the former to the amino groups in the latter upon heating at 60°C [36]. In this study, PPF contains much Klason lignin (Fig. 2.1), but it might contain certain amount of protein because PPF is fruit fiber. These proteins potentially lead to browning by Maillard reaction with heating during cellulose purification.

Fig. 2.3. The CNF sheets obtained from the palm pressed fiber (a), empty fruit bunch (b), palm kernel shell (c), and trunk (d).

Fig. 2.4 shows the results of AFM observation for the surface of the CNF sheets. The CNFs from the PPF, EFB, and PKS were reasonably nano-fibrillated, but fiber bundles remained (Fig. 2.4-a, b, c). Especially for PKS, many fiber bundles were observed. Thick fiber bundles remained on the surface of the PPF CNF sheet. On the other hand, the CNF from the trunk was uniformly nano-fibrillated. These results indicate that the cellulose pulp from the

trunk can be nano-fibrillated more easily than that from other parts of the plant. It has been reported that cellulose pulp from plants with high cellulose content, which means little other matrix substances in cell walls, was difficult to nano-fibrillate uniformly [14]. Among these matrix substances, hemicelluloses show an important role in the nano-fibrillation of wood pulp [37]. Hemicelluloses located between microfibrils inhibit their coalescence; that is, hemicelluloses prevent the strong hydrogen-bonding between the nanofiber bundles [37]. In this study, hemicellulose contents of PPF, EFB, and PKS were lower than that of the trunk (Fig. 2.1). These cell wall compositional differences in the raw materials might influence the ease of nano-fibrillation of the cellulose pulp.
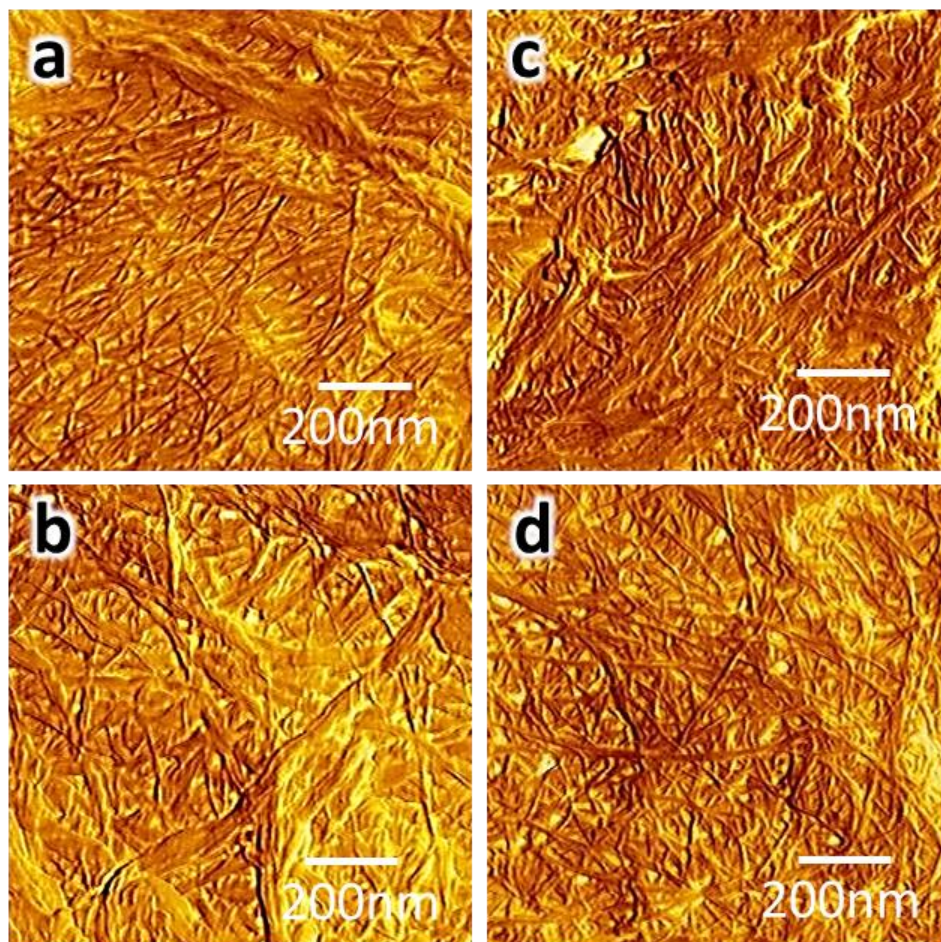

Fig. 2.4. AFM images of the surface of CNF sheets obtained from the palm pressed fiber (a), empty fruit bunch (b), palm kernel shell (c), and trunk (d).

Chapter 2

2.3.3. Degree of crystallinity and crystallite size of sheets

The XRD patterns were obtained to determine the crystalline index of the CNF sheets (Fig. 2.5). All CNF sheets belonged to cellulose I_β, which is typical for natural plant cellulose, and chemical treatments did not affect the crystallites of the cellulose of any samples [16]. For PPF and PKS, a sharp peak was observed (Fig. 2.5-black arrow). These sharp peaks can be characterized as quartz [38]. This result suggests the presence of silica in these CNF samples [38].

Table 2.2 shows the degree of crystallinity and the crystallite size for the (200) diffraction plane of cellulose I of the CNF sheets calculated from the X-ray diffraction peak profiles. It was revealed that the crystallinity changed depending on the type of raw material, while the crystallite size was stable among all samples. Cellulose crystallinity of the CNF sheet from the PPF and PKS had lower crystallinity, and the highest crystallinity of 77.0% was exhibited by the sheet from the trunk. These differences might originate from the cell wall structures of the raw materials. It was reported that the degree of polymerization (DP) of cellulose obtained from primary cell walls was 5940, while that from secondary cell wall was 10650. Moreover, the existence of ultrafine cellulose microfibrils has been reported in fruit tissues. Cellulose obtained from the PPF, as fruit tissues consist mainly of primary cell walls, might be more sensitive to chemical and mechanical treatment because of their lower DP and thinner form, and thus, the crystallinity of the CNF sheet was possibly degraded.

On the other hand, these results suggest that cellulose from the PPF and PKS has an advantage in the production of fermentable sugars to make biofuels. Reduction of cellulose crystallinity in pretreatment processes can significantly improve the hydrolysis by cellulose enzymes. There have been many reports already on the production of biofuels from EFB. The

author recommends further studies on the production of biofuels from PPF and PKS, in addition to EFB.
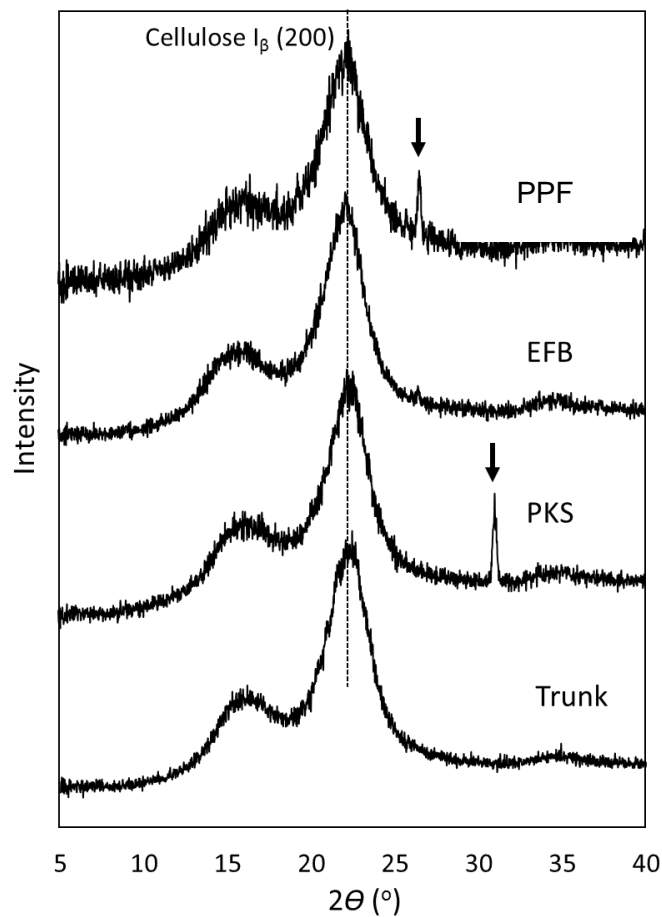
Fig. 2.5. X-ray diffraction profiles of CNF sheets obtained from the palm pressed fiber, empty fruit bunch, palm kernel shell, and trunk.

Table 2.2. Crystallinity and crystallite size of the CNF sheets obtained from palm pressed fiber, empty fruit bunch, palm kernel shell, and trunk.

Sample	Crystallinity (%)	Crystallite size (Å)
Palm pressed fiber	69.1	29.8
Empty fruit bunch	74.9	30.5
Palm kernel shell	71.1	30.6
Trunk	77.0	28.6

2.3.4. Thermal degradation properties of sheets

TG curves showed the weight loss of the CNF sheets upon heating (Fig. 2.6). The thermal decomposition occurred at higher temperatures in PPF and PKS, while the 5% weight loss temperatures of EFB and Trunk were 297 and 274°C, respectively. The lower thermal stability may be due to the successful of nano-fibrillation of EFB and trunk cellulose fibers. It was reported that the thermal stability of the microfibrillated cellulose decreased after homogenization [45]. Increasing the contacts between cellulose microfibrils promoted dehydration reactions of cellulose, leading to the release of water and catalyzed nanocrystal decomposition.

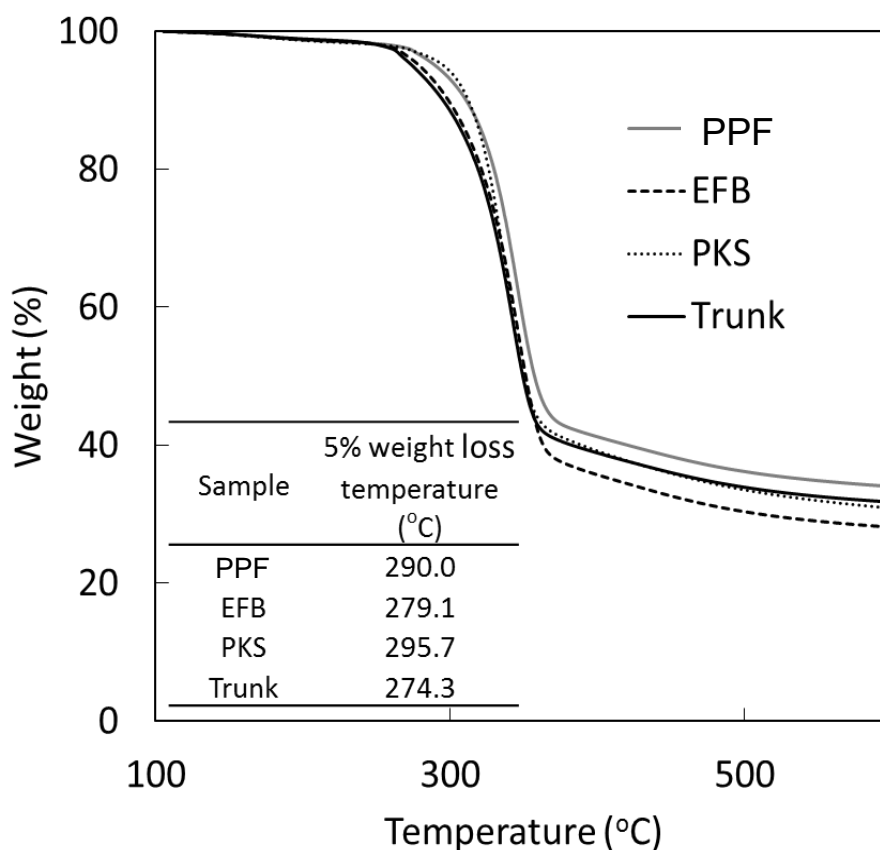| Sample	5% weight loss temperature (^{o}C)
PPF	290.0
EFB	279.1
PKS	295.7
Trunk	274.3

Fig. 2.6. Thermogravimetric (TG) curves of the CNF sheets obtained from palm pressed fiber, empty fruit bunch, palm kernel shell, and trunk.

Chapter 2

In addition, other reports suggested that the smaller size of cellulose nanocrystals provided a larger accessible surface area for heat treatment [20]. In this study, CNF obtained from PPF could not have been nano-fibrillated uniformly because CNF sheet from PPF was not transparent (Fig. 2.3). Many fiber bundles were observed on the surface of CNF sheets obtained from PKS (Fig. 2.4-c). These morphological differences might affect their heat resistance.

2.3.5   Mechanical properties of sheets

A tensile test was performed for each CNF sheet, and stress-strain curves are plotted in Fig. 2.7. There was a clear difference among the stress–strain behavior of each sample. The value of specific tensile strength and specific Young's modulus were highest in the CNF sheet of the trunk (Table 2.3). On the other hand, lowest mechanical properties shown in the CNF sheet from the PPF. The CNF sheets obtained from the PKS show brittle and fragile behavior such as low tensile strength and strain. These results were well in agreement with the results of the degrees of crystallinity of the CNF sheets (Table 2.2). The decrease of the degree of crystallinity corresponds to the lowering of the elasticity of the cellulose fibers, which causes the decrease of the Young's modulus of the sheets [37]. In addition, the microfibrillation enhances the tensile strength when the film is dried because of the stronger hydrogen bonding on the larger surface areas of the microfibrils [10]. In this study, it was suggested that the most successful uniform nano-fibrillation was obtained from trunk cellulose fibers, as the CNF sheets obtained from the trunk showed the highest mechanical properties.
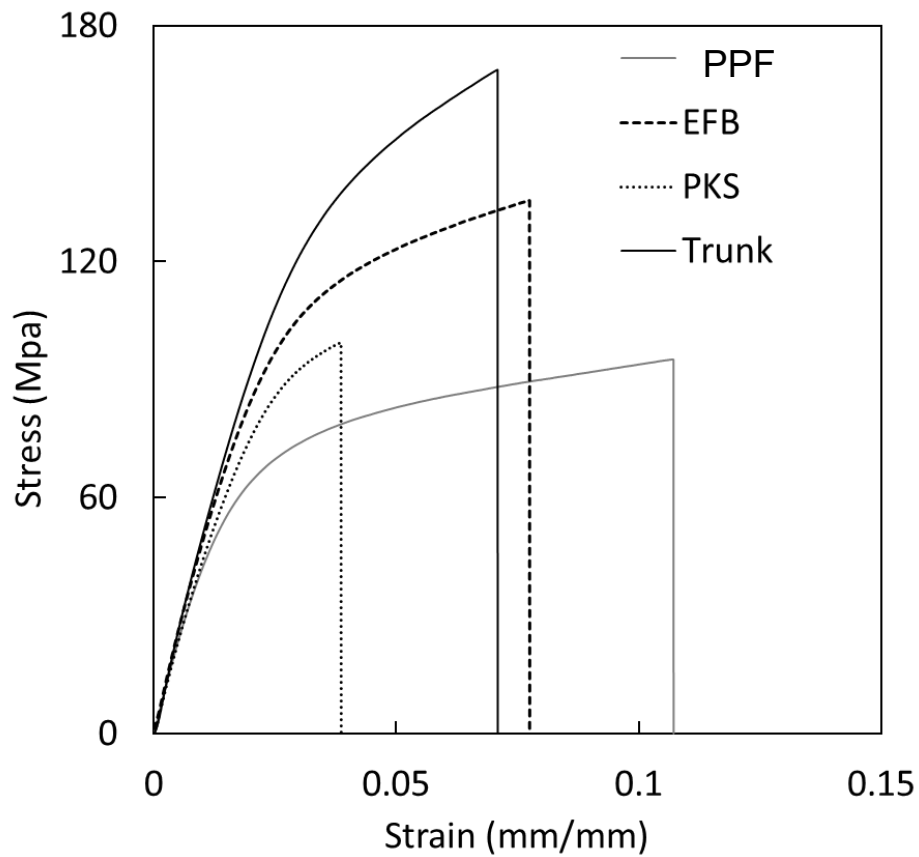
Fig. 2.7. Stress-strain curves of CNF sheets obtained from the palm pressed fiber, empty fruit bunch, palm kernel shell, and trunk.

Table 2.3. Mechanical properties of the CNF sheets obtained from the palm pressed fiber, empty fruit bunch, palm kernel shell, and trunk.

Sample	Density (g/cm^3) ρ	Specific tensile strength (Mpa) σ_{max}/ρ	Specific tensile strain (%) ε_{max}/ρ	Specific Young's modulus (Gpa) E/ρ
Palm pressed fiber	0.98	95 ± 9	10.8 ± 1.8	3.5 ± 0.6
Empty fruit bunch,	1.00	119 ± 7	8.1 ± 1.6	4.1 ± 0.4
Palm kernel shell	1.02	103 ± 2	4.2 ± 0.4	4.3 ± 0.3
Trunk	0.96	157 ± 9	8.4 ± 1.1	5.0 ± 0.3

Chapter 2

2.4.   Conclusion

The chemical composition of the PPF, EFB, PKS, and trunk of oil palm trees varied; the hemicellulose content of the PPF was much lower than others while the lignin content of the PKS was much higher than others. However, the production of the CNF from all parts of the oil palm was achieved in this work. The morphology and mechanical properties of the CNF sheets obtained from the trunk had many advantages over the CNF sheets from other parts, but showed deteriorated thermal degradation properties. The crystallinity and mechanical properties of the CNF sheets from the PPF and PKS were much lower than those of the EFB and trunk. The degree of polymerization, structure, morphology, and surface properties of the resulting CNF can be very different depending on the raw materials. PPF, EFB, PKS, and trunk have different cell wall structures and chemical components from each other. It could lead to the differences of susceptibility to the treatment. For example, the PPF and PKS were obtained from the fruit tissues of the oil palm. These might have higher sensitivity to chemical and mechanical treatment than cellulose obtained from the trunk and EFB, so mild pretreatment might be required for the PPF and PKS. It is an expectation of the authors that these results will open up many possibilities for the new application of oil palm wastes.

Chapter 2

References

[1]   Sreekala, M., Kumaran, M., and Thomas, S.; Oil palm fibers: morphology, chemical composition, surface modification, and mechanical properties, *Journal of Applied Polymer Science*, 66, 821–835 (1997)

[2]   Awalludin, M. F., Sulaiman, O., Hashim, R., and Nadhari, W. N. A. W.; An overview of the oil palm industry in Malaysia and its waste utilization through thermochemical conversion, specifically via liquefaction, *Renewable and Sustainable Energy Reviews*, 50, 1469–1484 (2015)

[3]   Sabil, K. M., Aziz, M. A., Lal, B., and Uemura, Y.; Effects of torrefaction on the physiochemical properties of oil palm empty fruit bunches, mesocarp fiber and kernel shell, *Biomass and Bioenergy*, 56, 351–360 (2013)

[4]   Palamae, S., Dechatiwongse, P., Choorit, W., Chisti, Y., and Prasertsan, P.; Cellulose and hemicellulose recovery from oil palm empty fruit bunch (EFB) fibers and production of sugars from the fibers, *Carbohydrate Polymers*, 155, 491–497 (2017)

[5]   Siró, I., and Plackett, D.; Microfibrillated cellulose and new nanocomposite materials: a review, *Cellulose*, 17, 459–494 (2010)

[6]   Menon, M, P., Selvakumar, R., Kumar, P. S., and Ramakrishna, S.; Extraction and modification of cellulose nanofibers derived from biomass for environmental application, *RSC Advances*, 7, 42750–42773 (2017)

[7]   Klemn, D., Kramer, F., Moritz, S., Lindström, T., Ankerfors, M., Gray, D., and Dorris, A.; Nanocelluloses: A new family of nature-based materials, *Angewandte Chemie International Edition*, 50, 5438–5466 (2011)

[8]   Isogai, A.; Wood nanocelluloses: fundamentals and applications as new bio-based nanomaterials, *Journal of Wood Scienc*e, 59, 449–459 (2013)

Chapter 2

[9]   Dufresne, A., Cavaille, J., and Vignon, M.; Mechanical behavior of sheets prepared from sugar beet cellulose microfibrils, *Journal of Applied Physics*, 64, 1185–1194 (1997)

[10]   Taniguchi, T., and Okamura, K.; New films produced from microfibrillated natural fibres, *Polymer International*, 47, 291–294 (1998)

[11]   Iwamoto, S., Nakagaito, A. N., Yano, H., and Nogi, M.; Optically transparent composites reinforced with plant fiber-based nanofibers, *Applied Physics A*, 81, 1109–1112 (2005)

[12]   Abe, K., Iwamoto, S., and Yano, H.; Obtaining cellulose nanofibers with a uniform width of 15 nm from wood, *Biomacromolecules*, 8, 3276–3278 (2007)

[13]   Alemdar, A., and Sain, M.; Biocomposites from wheat straw nanofibers: Morphology, thermal and mechanical properties, *Composites Science and Technology*, 68, 557–565 (2008)

[14]   Chen, W., Yu, H., Liu, Y., Hai, Y., Zhang, M., and Chen, P.; Isolation and characterization of cellulose nanofibers from four plant cellulose fibers using a chemical-ultrasonic process, *Cellulose*, 18, 433–442 (2011)

[15]   Puangsin, B., Yang, Q., Saito, T., and Isogai, A.; Comparative characterization of TEMPO-oxidized cellulose nanofibril films prepared from non-wood resources, *International Journal of Biological Macromolecules*, 59, 208–213 (2013)

[16]   Nobuta, K., Teramura, H., Ito, H., Hongo, C., Kawaguchi, H., Ogino, C., Kondo, A., and Nishino, T.; Characterization of cellulose nanofiber sheets from different refining processes, *Cellulose*, 23, 403–414 (2016)

[17]   Solikhin, A., Hadi, Y. S., Massijaya, M. Y., and Nikmatin, S.; Nanostructural, chemical, and thermal changes of oil palm empty fruit bunch cellulose nanofibers pretreated with different solvent exetractions, *Waste and Biomass Valorization*, 10, 953–965 (2019)

Chapter 2

[18] Fahma, F., Iwamoto, S., Hori, N., Iwata, T., and Takemura, A.; Isolation, preparation, and characterization of nanofibers from oil palm empty-fruit-bunch (OPEFB), *Cellulose*, 17, 977–985 (2010)

[19] Jonoobi, M., Khazaeian, A., Tahir, P. M., Azry, S. S., and Oksman, K.; Characteristics of cellulose nanofibers isolated from rubberwood and empty fruit bunches of oil palm using chemo-mechanical process, *Cellulose*, 18, 1085–1095 (2011)

[20] Chieng, B. C. W., Lee, S. H., Ibrahim, N. A., Then, Y. Y., and Loo, Y. Y.; Isolation and characterization of cellulose nanocrystals from oil palm mesocarp fiber, *Polymer*, 9, 1–11 (2017)

[21] Lamaming, J., Hashim, R., Leh, C. P., and Sulaiman, O.; Properties of cellulose nanocrystals from oil palm trunk isolated by total chlorine free method, *Carbohydrate Polymers*, 156, 409–416 (2017)

[22] Su, Y., Burger, C., Ma, H., Chu, B., and Hsiao, B. S.; Morphological and property investigations of carboxylated cellulose nanofibers extracted from different biological species, *Cellulose*, 22, 3127–3135 (2015)

[23] Elazzouzi, S., Nishiyama, Y., Putaux, J., Heux, L., Dubreuil, F., and Rochas, C.; The shape and size distribution of crystalline nanoparticles prepared by acid hydrolysis of native cellulose, *Biomacromolecules*, 9, 57–65 (2008)

[24] Shibata, M., Varman, M., Tono, Y., Miyafuji, H., and Saka, S.; Characterization in chemical composition of the oil palm (*Elaeis guineensis*), *Journal of the Japan Institute of Energy*, 87, 383–388 (2008)

[25] Loader, N. J., Robertson, I., Barker, A. C., Switsur, V. R., and Waterhouse, J. S.; An improved technique for the batch processing of small whole wood samples to α-cellulose, *Chemical Geology*, 136, 313–317 (1997)

Chapter 2

[26] Wise, L. E. and Ratliff, E. K.; Quantitative isolation of hemicelluloses and summative analysis of wood, *Analytical Chemistry*, 19, 459–462 (1947)

[27] Dence, C. W.; The determination of lignin, In S. Y. Lin, and C. W; Dence (Eds.). *Methods in Lignin Chemistry* (pp. 33–61). Berlin, Heidelberg: Springer (1992)

[28] Bunzel, M., Schüssler, A., and Tchetseubu Saha, G.; Chemical characterization of Klason lignin preparations from plant-based foods, *Journal of Agricultural and Food Chemistry*, 59, 12506–12513 (2011)

[29] Segal, L., Creely, J. J., Martin, A. E., and Conrad, C. M.; An empirical method for estimating the degree of crystallinity of native cellulose using the X-ray diffractometer, *Textile Research Journal*, 29, 786–794 (2016)

[30] Alexander, L. E.; *X-ray Diffraction Methods in Polymer Science.* New York: John Wiley and Sons, (Chapter 7) (1969)

[31] Reyes, J., Gonzalo Canché, G., Soto, M., and Terrazas, T.; Wood chemical compo-sition in species of cactaceae: the relationship between lignification and stem morphology, *PLoS ONE*, 10, e0123919 (2015)

[32] Xu, F., Yu, J., Tesso, T., Dowell, F., and Wang, D.; Qualitative and quantitative analysis of lignocellulosic biomass using infrared techniques: A mini-review, *Applied Energy*, 104, 801–809 (2013)

[33] Sene, C., McCann M., Wilson, R., and Grinter, R.; Fourier-transform raman and fourier-transform infrared, *Plant Physiology*, 106, 1623–1631 (1994)

[34] Ogawa, H., Ishikawa, K., Inomata, C., and Fujimura, S.; Initial stage of native oxide growth on hydrogen terminated silicon (111) surfaces, *Journal of Applied Physics*, 79, 472–477 (1996)

[35] Nogi, M., Iwamoto, S., Nakagaito, A. N., and Yano, H.; Optically transparent nanofiber paper, *Advanced Materials*, 21, 1595–1598 (2009)

Chapter 2

[36] Elzoghby, A. O., Elgohary, M. M., and Kamel, N. M.; Implications of protein- and peptide-based nanoparticles as potential vehicles for anticancer drugs, Chapter 6 *Advances in Protein Chemistry and Structural Biology*, 98, 169–221 (2015)

[37] Iwamoto, S., Abe, K., Yano, H.; The effect of hemicelluloses on wood pulp nanofibrillation and nanofiber network characteristics, *Biomacromolecules*, 9, 1022–1026 (2008)

[38] Lanning, F., Ponnaiya, B., and Crumpton, C.; The chemical nature of silica in plants, *Plant Physiology*, 33, 339–343 (1958)

[39] Hessler, L., Merola, G., and Berkley, E.; Degree of polymerization of cellulose in cotton fibers, *Textile Research Journal*, 18, 628–634 (1948)

[40] Niimura, H., Yokoyama, T., Kimura, S., Matsumoto, Y., and Kuga, S.; AFM observation of ultrathin microfibrils in fruit tissues, *Cellulose*, 17, 13–18 (2009)

[41] McMillan, J. D.; Pretreatment of lignocellulosic biomass. In Himmel, M.E., Baker, J. O., Overend, R.P. (Eds.), *Enzymatic Conversion of Biomass for Fuels Production* (p.p. 292–324). Washington, DC, American Chemical Society (1994)

[42] Cui, X., Zhao, X., Zeng, J., Loh, S. K., Choo, Y. M., and Liu, D.; Robust enzymatic hydrolysis of Formiline-pretreated oil palm empty fruit bunches (EFB) for efficient conversion of polysaccharide to sugars and ethanol, *Bioresource Technology*, 166, 584–591 (2014)

[43] Hassan, O., Ling, T. P., Maskat, M. Y., Illias, R. M., Badri, K., Jahim, J., and Mahadi, N. M.; Optimization of pretreatments for the hydrolysis of oil palm empty fruit bunch fiber (EFBF) using enzyme mixtures, *Biomass and Bioenergy*, 56, 137–146 (2013)

[44] Kim, S., and Kim, C. H.; Bioethanol production using the sequential acid/alkali-pretreated empty palm fruit bunch fiber, *Renewable Energy*, 54, 150–155 (2013)

Chapter 2

[45] Piarpuzán, D., Quintero, J. A., and Cardona, C. A.; Empty fruit bunches from oil palm as a potential raw material for fuel ethanol production, *Biomass and Bioenergy*, 35, 1130–1137 (2011)

Chapter 3

Relationships between Dyeing Conditions
and Dyeability of Extracts from Oil Palm Tree

3.1.   Introduction

The African oil palm tree (*Elaeis guineensis*) is one of the plants belonging to oil palm genus and vegetable oil is obtained from oil palm trees. Palm oil gained from oil palm is used as food oil, processed food products, detergents, lubricant oil, fuel and so on. The production amount of palm oil in the world is 74 million metric tons (2018/19) [1], of which amount is the best in the world, and it increases year by year. The amount of palm tree wastes after the expression of oil increases with an increase in the oil production. A huge amount of waste left over from the production of oil causes problems [2]. It is important to reutilize the waste in order to solve the problems. Some of the oil palm wastes are converted into organic fertilizers, animal feedstock and soil conditioner, and their direct combustion, gasification, pyrolysis and liquefaction have been attempted [2]. On the other hand, a trial to harvest cellulose nanofibers from the oil palm wastes was made and their morphological, thermal and mechanical properties were studied in Chapter 2. The study showed a possibility for the effective use of the waste.

Plants often contain a variety of useful component compounds and some of them work as dyestuffs for fiber materials. One of the authors studied the dyeability of the extracts from mulberry (*Morus*) branches and trunks for wool, silk, cotton, ramie, nylon, acrylic, and polyester fabrics [3]. The mulberry branches and trunks are also wastes after used for sericulture to produce silk fibers. It was found that wool, nylon, and silk fabrics are dyed brownish and yellowish colors by the water-extracts from mulberry branches and trunks, and moreover the extracts show fluorescence and reducing property. The peels

Chapter 3

of black mulberry (*Morus nigra*) were used to, for example, colour woods [4]. Colourant ingredients were extracted from the peels with water in an ultrasonic bath and wood samples were coloured brown.

The water-extracts from the oil palm tree might be able to serve fiber materials as dye. The exploitation and development of novel sustainable dyestuffs and the effective utilisation of plant wastes are significant to establish a sustainable society. The authors have not found information on a scientific study of dyeing by using extracts from oil palms. Therefore, it can be said that dyeing of fabrics by using a dyestuff obtained from the wastes of oil palm tree has not been studied aiming to apply the dyestuff to industrial uses. There are advantages to obtain a dyestuff from oil palm trees and use it. An expected great advantage is that the dyestuff can be obtained as the by-product of palm oil. The remnants after the dye-extraction are used as the raw materials for cellulose products, such as cellulose nano-fibre films and resins. This means an effective utilisation of oil palm trees. It is a distinctive point of oil palm trees that they work as the resources for oil, dyestuffs and cellulose. Furthermore, a large quantity of dyestuffs can be produced and the cost may be able to be lowered because the amount of oil palm tree wastes increases considerably in the world with an increase of the palm oil production. The low price of the oil palm extracts contributes to the popular use of the natural dyestuffs in industrial production.

Under such the situation, the authors tried to dye fabrics with extracts from an oil palm tree in the study. It is a great advantage to take dyestuffs from oil palm trees, because the residues after the extraction can be utilised as the source of cellulose and the dyestuff source is sustainable when oil palm trees are continuously cultivated in an appropriate environment.

Chapter 3

The parts of oil palm trees used in the chapter are the trunk, empty fruit bunch (EFB), palm pressed fiber (PPF), and palm kernel shell (PKS). The oil is taken from the fruit and kernel. The materials used in the study were obtained after the oil production.

In the first place, the dyeability of the extracts from each of the parts for silk fabric was examined. Secondly, the dependences of dyeability for silk fabric on the extracts concentration in dyeing solution, dyeing time or dyeing temperature were investigated. Thirdly, the dyeability of the extracts for natural fibres such as wool, cotton, ramie, and synthetic fibres such as acrylic, polyester, nylon was evaluated.

3.2. Materials and Methods

3. 2.1 Extraction from oil palm tree

The sample oil palm trees (*Elaeis guineensis – Tenera*) were obtained from Suksomboom Palm Oil Co., Ltd (Chonburi, Thailand). The trees were ten years old and each of the parts was dried in the sun after palm oil expressed. The obtained parts were separated and classified into trunk, EFB, PPF, and PKS (Fig. 2.1). They were crashed and ground up into powder with a mill (Osaka Chemical Co. Wonder Blender WB-1). Each of the powders placed in a Soxhlet's extractor was extracted with distilled water at 100°C for 14 h. The extract solutions were concentrated with a rotary evaporator and dried under reduced pressure. The dried solids were ground into powder.

3.2.2. Fabrics

The silk fabric (Kinu Habutai, Shikisensha, basis weight: 52.5 gm^{-2}, yarn density: 135×98 per inch, warp yarn count: 31, weft yarn count: 21, plain weave), wool fabric (Tropical, Shikisensha, basis weight: 180 gm^{-2}, yarn density: 69.5×58 per inch, warp yarn count: 60/2, weft yarn count: 60/2, plain weave), cotton fabric (Broad,

Chapter 3

Shikisensha, basis weight: 122 gm^{-2}, yarn density: 130 × 70 per inch, warp yarn count: 40/1, weft yarn count: 40/1, plain weave), ramie fabric (Broad, Shikisensha, Shikisensha, basis weight: 91 gm^{-2}, yarn density: 52 × 56 per inch, warp yarn count: 60/1, weft yarn count: 60/1, plain weave), acrylic fabric (Muslin, Shikisensha, basis weight: 107 gm^{-2}, yarn density: 68 × 58 per inch, warp yarn count: 52/1, weft yarn count: 52/1, plain weave), polyester fabric (Tafta, Shikisensha, basis weight: 71.8 gm^{-2}, yarn density: 120 × 90 per inch, warp yarn count: 75 d × 36 f, weft yarn count: 75 d × 36 f, plain weave), nylon fabric (Tafta, Shikisensha, basis weight: 60.4 gm^{-2}, yarn density: 108 × 82 per inch, warp yarn count: 70 d × 12 f, weft yarn count: 70 d × 24 f, plain weave) were cut into 5 cm squares and used for the dyeing experiments. The fabric samples were washed with 2.0 wt% marseille soup solution at 40°C for 10 min, rinsed with distilled water at 40°C for 5 min three times and air-dried. The liquor ratio for washing with the marseille soap solution was 40:1 and that for rinsing was 100:1. The dried fabric samples were weighed and their masses were recorded for fixing the liquor ratio in dyeing procedure.

3.2.3. Dyeing

3.2.3.1 Dyeability of extracts from each of the parts

A fixed amount of extracts obtained from each of the parts (trunk, EFB, PPF, and PKS) was introduced into distilled water and stirred to prepare dyeing solution. The extracts were partly dissolved and dispersed. Therefore, the amount of extracts in the dyeing solution is expressed as $x_f = m_{EP} / m_w$ [g/g], where m_{EP} is the mass of extracts powder and m_w the mass of distilled water. Silk fabric was immersed into the extracts solution ($x_f = 0.020$), which contained minute amounts of the extracts powder as dispersoid and was prepared from trunk, EFB, PPF or PKS at 50°C for 180 min. The liquor ratio was 100:1 and the moving rate of incubator was 80 rpm. Each of the samples

Chapter 3

was washed with 50 ml of 2.0 wt% Marseille soup solution at 40°C for 5 min, rinsed with 100 ml of distilled water at 40°C for 5 min twice and air-dried.

3.2.3.2 Dependence of dyeability on x_f, time or temperature for silk fabric

A fixed amount of PKS extracts was introduced into distilled water and stirred to prepare dyeing solution. The x_f was varied from 0.0010 to 0.020 in the experiments to investigate the relationship between the amount of PKS extracts in dyeing solution and the dyeability. The amounts of extracts supplied in the dyeing solution were comparatively large, because the liquor ratio employed was high and the content rate of effective dyestuffs in the extracts and the disability had not been unknown. Silk fabric was immersed into the extracts solution at 60°C for 180 min. The liquor ratio was 100:1 and the moving rate of incubator was 100 rpm.

The dyeing time (t) was altered from 30 min to 360 min to obtain data for the time dependence of the dyeability. The x_f was 0.010 and other dyeing conditions except the time were the same as the x_f dependence experiments.

The dyeing temperature (T) was controlled as 40, 50, 60, 70, and 80°C for the temperature dependence of the dyeability. The x_f was 0.010 and other dyeing conditions except the temperature were the same as the x_f dependence experiments.

Each of the samples was washed with 50 ml of 2.0 wt% Marseille soup solution at 40°C for 5 min, rinsed with 100 ml of distilled water at 40°C for 5 min twice and air-dried.

3.2.3.3 Dyeability of natural and synthetic fibers

Wool, cotton, ramie, acrylic, polyester and nylon fabrics were dyed under same conditions as $x_f = 0.010$, liquor ratio: 100:1, t: 180 min, T: 60°C, and washed rinsed and dried as previously described.

Chapter 3

3.2.4   Color measurements

The obtained colour of the fabric samples was measured by using a spectrocolorimeter (Konica Minolta CM-2600d) and the resulting colour was expressed in $L^*a^*b^*$ standard colorimetric system (CIE 1976). The colour measurements were made employing CIE standard illuminant D_{65}, 10°-view angle and SCI (specular component included) mode. All the reflected lights from the sample including the regular reflection are integrated under the SCI mode. The a^* and b^* are the chromaticity coordinates, and L^* is the lightness index in the $L^*a^*b^*$ system. The positive values of a^* indicate reddish colours and the negative values of that indicate greenish ones, and the positive values of b^* indicate yellowish and the negative values indicate bluish. The C^* is the chroma calculated as $C^* = \{(a^*)^2 + (b^*)^2\}^{1/2}$ [5,6].

The color strength is generally estimated by using K/S value, which was defined from Kubelka-Munk theory [7,8]. It is calculated by using a reflectance value at a wavelength λ as $K/S_\lambda = (1 - R_\lambda)^2/2R_\lambda$, where K is the absorption coefficient, S the scattering coefficient and R_λ the reflectance of the light at a wavelength λ. Higher K/S value indicates higher strength of a colour, i.e., deeper colour or higher optical density of colour. The measurement of sample colours was conducted at five points of each sample (diameter of measured circle: 8 mmϕ). The arithmetic mean was calculated from the obtained values excluding outliers.

3.3   Results and Discussion

3.3.1   Dyeability of extracts from each of the parts

Brown ~ yellowish brown powders are obtained by the extraction from the parts of the oil palm tree with water. The yield of extracts obtained from PKS for 14 h extraction

Chapter 3

is 2.20 wt%. The obtained colours of the silk fabric treated with trunk, EFB, PPF or PKS are very pale orange, pale grey, grey or brownish orange, respectively. This shows that the extracts from PKS obtained with water dye effectively silk brownish orange. The obtained color data expressed in lightness index L^* and chromaticity coordinates a^* and b^* values for the silk fabrics are summarised in Table 3.1. The silk fabric sample treated with PKS extracts shows lowest L^* value and highest a^*, b^* values. The results represent that while trunk, EFB and PPF extracts are not effective dyestuffs when they are used without combining with an extra treatment, PKS extracts work as dyestuff and dye silk deepest colour with high chroma.

Table 3.1.   The obtained color data expressed in L^*, a^*, and b^*.

Sample	L^*	a^*	b^*
Silk before treatment	84.9	-3.30	9.31
Silk treated with trunk extracts	79.8	4.10	20.0
Silk treated with empty fruit bunch extracts	70.0	3.96	13.1
Silk treated with palm pressed fiber extracts	61.2	5.55	16.1
Silk treated with palm kernel shell extracts	59.4	17.4	45.8

L^*, a^*, and b^* values obtained for silk fabrics before treatment, treated with trunk extracts, with empty fruit bunch extracts, with palm pressed fiber extracts and with palm kernel shell extracts. Samples were dyed with $x_f = 0.020$ at 50°C for 180 min.

The phenolic compounds in oil palm extracts, which were extracted with ethanol/water mixture (solvent volume ratio in mixing was ethanol : water = 7 : 3)

Chapter 3

containing HCl, were analysed [9]. The extracts were taken from palm kernel cake (PKC), EFB, palm pressed fiber (PPF) or PKS in this paper. PKC was not used in Chapter 2 and hence the results for the extracts from EFB, PPF, and PKS are compared here. The characteristics of the chemical composition of the extracts from PKS is that they contain pyrogallol, vanillin, and sinapinic acid, which were not found in the extracts from EFB and PPF and they include more amount of catechins than the extracts from EFB and PPF. The phenolic compounds show reducing property and they are oxidised. The colourants and phenolic dye precursors are oxidised to give a lot of kinds of dyestuffs during extracting and dyeing processes as mentioned later on. The pyrogallol and catechins contained in the extracts from PKS should play an important role in the dyeing because catechins give dyestuff [10,11] and pyrogallol was once used as a coupler to form dyestuffs with dye precursors for controlling the obtaining color of human hair [12]. The pyrogallol and catechins have many phenolic hydroxyl groups in their molecules and proceed oxidation and coupling reactions to give colorants. Based on these results, PKS extracts were used in dyeing experiments reported hereinafter.
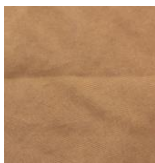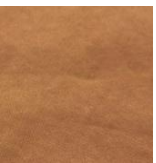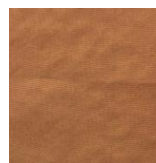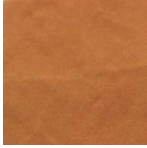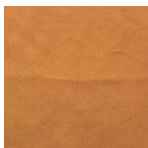
3.3.2 Dependence of silk fabric dyeability on x_f

The silk fabric sample was dyed by PKS extracts with increasing x_f (the amount of extracts in the dyeing solution) at 60°C for 180 min. The colours of resulting silk samples are brown ~ brownish orange. The photographs of obtained dyed samples are shown in Table 3.2 in order to make it easier to recognize and understand the difference in color. The results show that silk is dyed decently deep brown even at low amount of PKS extracts as $x_f = 0.0010$ (10% o.w.f.). It can be said that the dyeability of PKS extracts for silk is high enough. L^*, a^*, and b^* values obtained are also shown in Table 3.2. L^* decreases with increasing x_f until $x_f \leq 0.0050$ and increases slightly up to $x_f = 0.020$. a^*

and b^* increases with increasing x_f. The plot of a^* and b^* as a function of x_f is shown in Fig. 3.1. The plot does not show a linear relationship and curves upward (in the direction of higher b^*) with an increase in x_f as shown in the figure. This demonstrates that the hue of the dyed silk changes with increasing the amount of extracts in the dyeing solution.

Table 3.2. L^*, a^*, and b^* values obtained for silk fabrics.

x_f	Before dyed	0.0010	0.0020	0.0050	0.0060
Silk					
L^*	96.0	53.7	51.5	46.1	46.6
a^*	-0.222	13.8	14.4	17.5	20.4
b^*	3.31	29.6	30.0	32.5	35.9

x_f	0.0075	0.010	0.015	0.020
Silk				
L^*	47.9	46.4	47.9	50.0
a^*	21.9	22.7	22.8	23.1
b^*	38.3	38.0	40.7	43.7

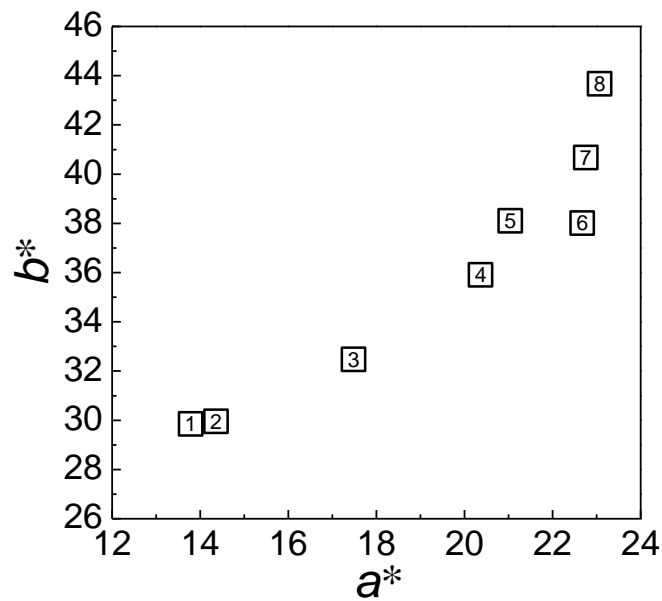Before dyed and dyed with each x_f and photographs of samples. Samples were dyed with at 60°C for 180 min.

Fig. 3.1. Color measurement results as shown by a^*-b^* relationships for silk fabric dyed with PKS extracts solution. Amount of extracts in the dyeing solution x_f = 0.0010: 1, 0.0020: 2, 0.0050: 3, 0.0060: 4, 0.0075: 5, 0.010: 6, 0.015: 7, 0.020: 8.

Fig. 3.2 (a) shows the K/S spectra of the dyed silk and the magnified view of the spectra from 480 to 560 nm is depicted in Fig. 3.2 (b). The spectral shapes are almost same and K/S values increase at $0.0010 \leq x_f \leq 0.0060$ and at $x_f = 0.010$, whereas they are different at $x_f = 0.0075$, 0.015 and 0.020. The spectra at $x_f = 0.0075$, 0.015, 0.020 and the spectra at $x_f = 0.0050$, 0.0060, 0.010 cross and show different optical characteristics. In fact, the plot of a^* and b^* shows a linear relationship for the data of $0.0010 \leq x_f \leq 0.0060$ and $x_f = 0.010$ in Fig. 3.1. It indicates that the dye molecules change chemically or interacts with one another during the dyeing to give the shift of the color. The experiments investigating the extracts in solution are described later at §3.5 in order to understand the results.
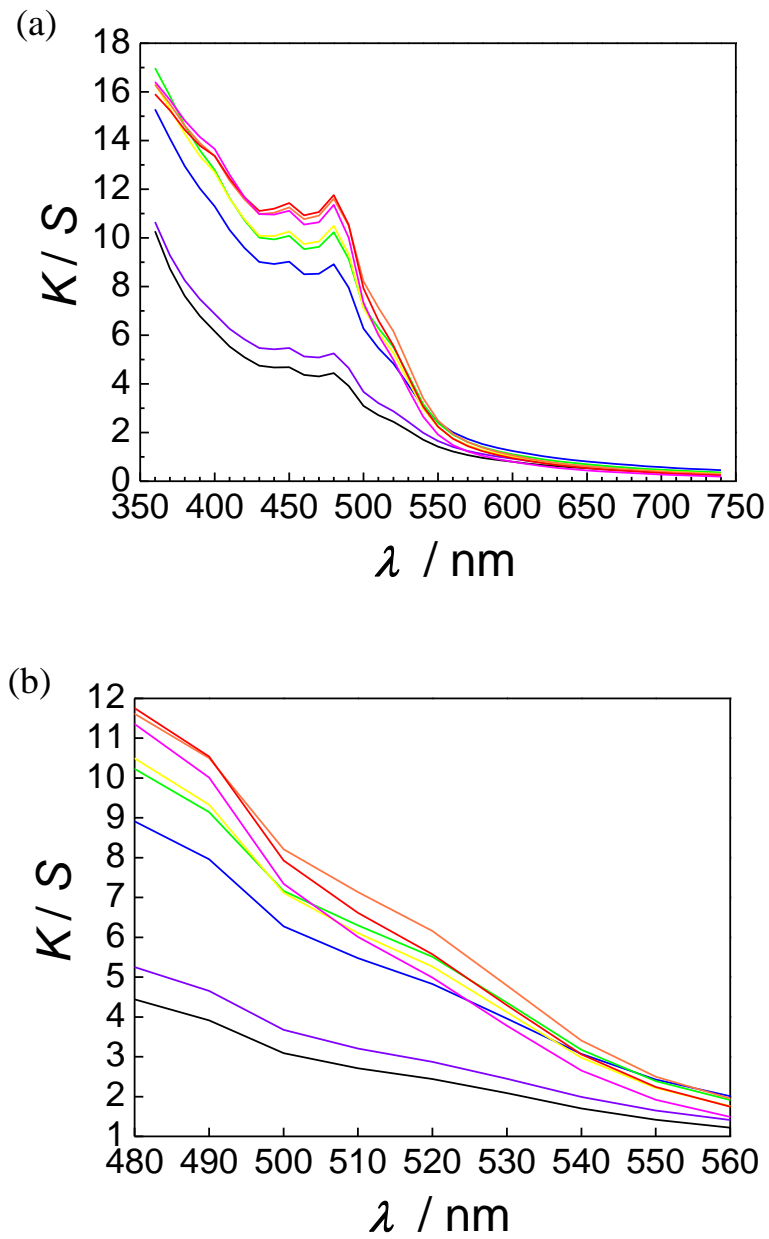
Fig. 3.2. *K/S* spectra of dyed silk with palm kernel shell extracts solution (a) and the magnified view of the spectra from 480 to 560 nm (b). x_f = 0.0010: ——, 0.0020: ——, 0.0050: ——, 0.0060: ——, 0.0075: ——, 0.010: ——, 0.015: ——, 0.020: ——.

Chapter 3

3.3.3   Dependence of silk fabric dyeability on dyeing time

It is important to obtain the information on the appropriate dyeing time for fixing the optimum time, by which enough and aimed color strength with practical levelness is obtained. Then, the dyeability of silk by PKS extracts was examined with changing dyeing time.

It was observed in the results that color of silk sample turns brownish orange and its deepness increases with dyeing time. Resulting L^*, a^*, and b^* values are shown in Table 3.3. L^* decreases with dyeing time t, a^* increases and b^* decreases slowly with t. The color obtained at 30 min of dyeing shows practical strength. Fig. 3.3 shows the K/S spectra of silk fabric dyed at each of t. The spectra show a shoulder peak at 480 nm of the wavelength and increase with t. The increase in K/S value is prominent at the peak and its vicinities. The pronounced crosses of the spectrum are not observed except the tiny ones at the short wavelength region. The results show that the color of silk dyed with PKS extracts changes slightly to reddish and increases in deepness with dyeing time.

Table 3.3. L^*, a^*, and b^* values obtained for silk fabrics.

t /min	Before dyed	30	60	120	150	180	240	300	360
L^*	96.0	59.5	55.9	50.8	48.2	46.4	45.2	44.0	42.3
a^*	-0.222	15.0	17.2	19.2	19.7	22.7	22.5	22.0	21.9
b^*	3.31	39.1	38.0	37.8	37.5	38.0	37.6	36.3	35.8

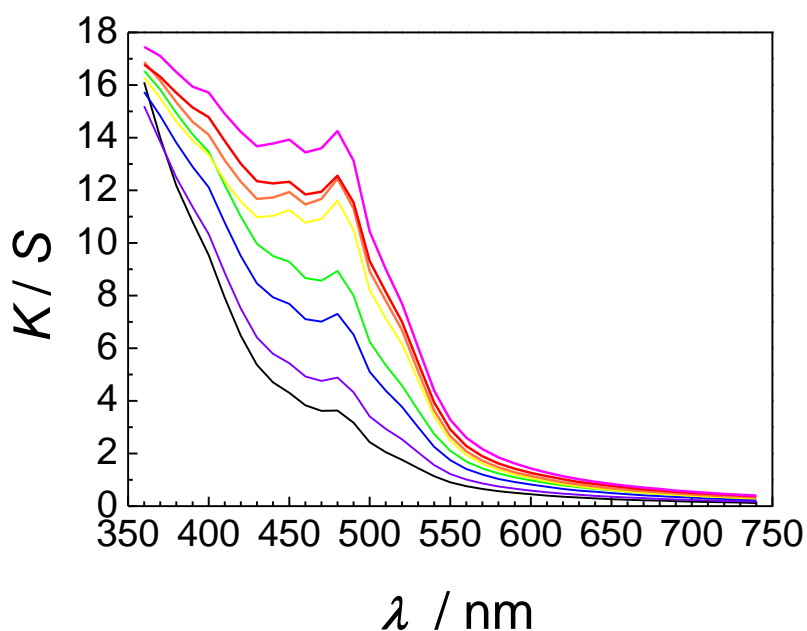Before dyed and dyed for each t. Samples were dyed with $x_f = 0.010$ at 60°C.

Fig. 3.3. *K/S* spectra of dyed silk with palm kernel shell extracts solution for *t* = 30

min: ——, 60 min: ——, 120 min: ——, 150 min: ——, 180 min: ——, 240

min: ——, 300 min: ——, 360 min: ——.

3.3.4   Dependence of silk fabric dyeability on dyeing temperature

Dyeing temperature usually influences significantly dyeability [13]. Therefore,

it is important to clarify the temperature dependence of the dyeability of PKS extracts.

Then, silk fabric samples were dyed at a series of temperature and obtained colors were

evaluated.

As a result, it was found that the brownish color of silk becomes darker with an

increase in the dyeing temperature *T*. Obtained *L**, *a**, and *b** values are shown in Table

3.4. *L** decreases with *T*, *a** increases with *T* at $T \leq 60°C$ and decreases at $T \geq 60°C$, and

b* increases at $T \leq 50°C$ and decreases at $T \geq 50°C$. These results show a general course

of change in colour of fibre samples dyed with increasing temperature. Furthermore, it is

understood that the silk is not dyed to saturation point, because the dyeing proceeds still

even at 80°C and L^* continues to decrease. In fact, The K/S values of the silk fabric increase with T from 70°C to 80°C as shown in the spectra of Fig. 3.4. The spectra show that the increase in K/S values in the region of ≤ 480 nm is especially remarkable. This also indicates that the chemical change of dye molecules during the dyeing process.

Table 3.4. L^*, a^*, and b^* values obtained for silk fabrics before dyed and dyed at each T.

T /°C	Before dyed	40	50	60	70	80
L^*	96.0	71.4	60.3	46.4	41.4	35.1
a^*	-0.222	11.8	16.0	22.7	20.1	17.5
b^*	3.31	41.6	43.7	38.0	34.0	24.1

Samples were dyed with $x_f = 0.010$ for 180 min.
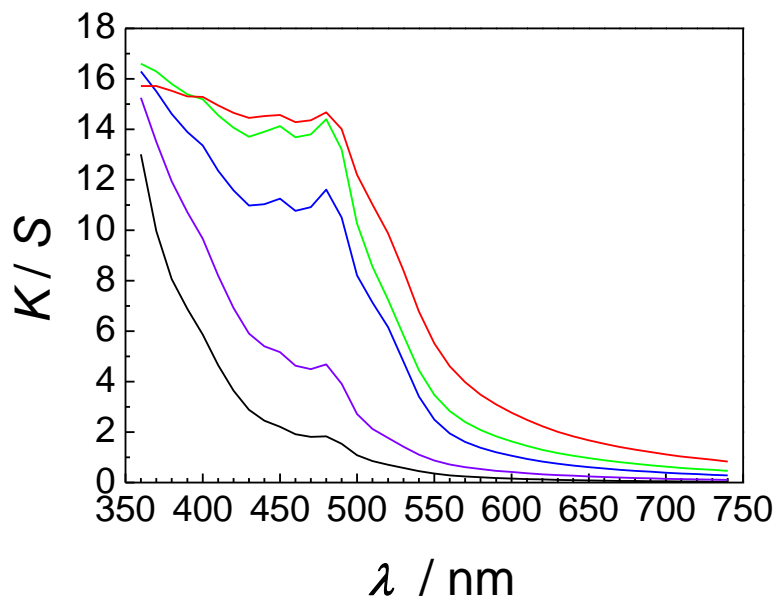

Fig. 3.4. K/S spectra of dyed silk with palm kernel shell extracts solution at $T =$ 40°C: ——, 50°C: ——, 60°C ——, 70°C: ——, 80°C: ——.

Chapter 3

The amount of dyestuffs adsorbed onto silk fibers and their distribution are strongly controlled by dyeing temperature. The dyeing rate increases with increasing temperature within a certain dyeing time [9]. Moreover, the sort and the composition of colorants adsorbed could be also changed by temperature if the dye molecules in the PKS extracts would be transformed. If the PKS extracts would contain the colorants, which work as reductants, their color should be changed by oxidation. The oxidation reaction of the colorants is promoted by heating in the presence of oxygen or air. Therefore, there is a possibility that the higher temperature during the dyeing accelerates the oxidation of the colorants contained in the extracts in addition to the effect of promotion of the diffusion rate of colorant molecules in silk fibers. Then, the solution spectra of PKS extracts were investigated as a first step. This is discussed at the next section.

On the hand, the color fastness of dyed fabrics is important property and practical products should show enough high fastness. The color fastness of for silk fabric dyed with PKS extracts to washing and light are being studied by the authors and will be reported.

3.3.5 Change in color of PKS extracts solution by heating

The PKS extracts aqueous solution ($x_f = 0.0010$) was prepared and filtered. The filtrate was allowed to stand at 40°C and 60°C for 180 min under air atmosphere in order to observe a change of colourants at the temperatures. As a result, it was found that the brownish colour of the solution turns darker as compared with that of the solution before heating. The change in colour of the sample heated at 60°C is larger and the colour is deeper than that at 40°C. The absorption spectra measured by Hitachi U-3900H for the PKS extracts aqueous solutions are shown in Fig. 3.5. It is observed that the absorbance A of the spectrum before heating increases after 180 min heating and the spectrum shape

changes. The increase in *A* and the shape change for the sample heated at 60°C is larger than that at 40°C.
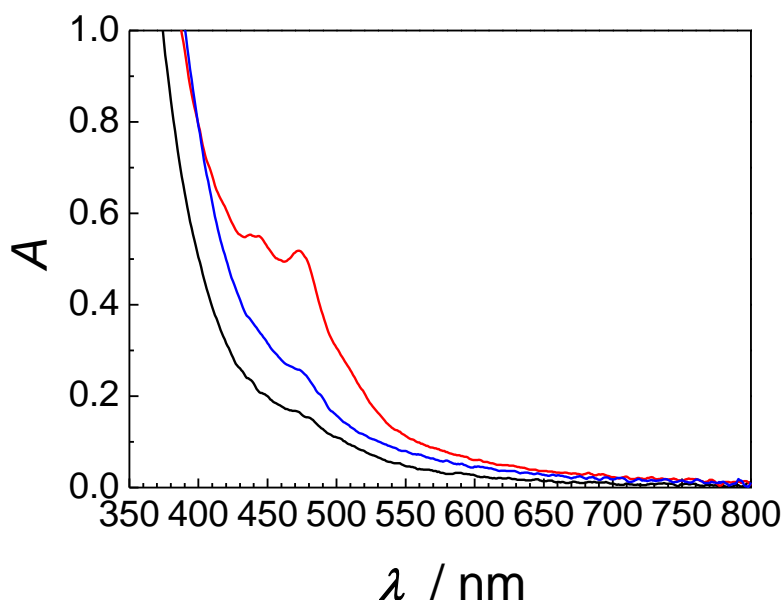

Fig. 3.5. Absorption spectra of palm kernel shell extracts aqueous solutions. Before heating: ——, heated at 40°C for 180 min: ——, 60°C for 180 min: ——.

The results indicate that chemical changes of colourant molecules take place in solution at 40 and 60°C. The color of flavonoids changes by oxidation [16] and turns into duller and/or darker one. Some phenolic molecules contained in PKS extracts can be oxidized by heating to give dye molecules showing different color. If fact, pyrogallol, catechins, 4-hydroxybenzoic acid, vanillin and sinapinic acid were found in PKS extracts as mentioned as has been explained above [9], and the extracts from fruits [15] and leaves [16] also show reducing property. The dyeing with increasing the amount of PKS extracts was made at 60°C as reported and discussed at §3.3.2. Therefore, the chemical change of dye molecules in solution may also be caused during the dyeing experiment. However, the changing manner of the K/S spectra shape for the x_f dependence system is somewhat

Chapter 3

different from that for the time and temperature dependence systems. The increase in K/S

values with increasing t and T is larger than that with increasing x_f. The chemical change

of dye molecules can proceed with increasing time and temperature. Meanwhile, another

effect such as aggregation of dyestuff molecules [17] also might contribute strongly to

the dyeability for the x_f dependence system. The aggregation induces the variation of the

dyestuff composition, which are adsorbed on the fibre. Anyhow, it can be said that the

colorants obtained in the extracts are "active" and change during dyeing processes. In the

study, the extraction was made by using distilled water and the color of extracts solution

deepened during the extraction and concentration procedures. It is not only by an increase

in the concentration of extracts in the solution but also the chemical change of extracts.

In fact, the color of the PKS extracts solution turned brown, when it was allowed to stand

in an air atmosphere. They mean that the powdered PKS extracts contain colorants formed

from the component substances such as pyrogallol, catechins, 4-hydroxybenzoic acid,

vanillin, sinapinic acid and/or etc. (+)-Catechin gives hair dyestuffs [10,14] and forms

dimers and multimers, some of which are colorant [18]. It was known that theaflavins are

formed from catechins in tea extracts solution [19,20] and they contribute to the brown

color of tea. Pyrogallol reacts with oxidized intermediates and yields dyestuffs as

mentioned. Therefore, it is thought that the dyestuffs in the PKS extracts consist of dye

molecules formed from pyrogallol, catechins and other ingredients and they are mixtures

of colorants. Further study should be made to clarify the mechanism.

3.3.6   Dyeability of natural and synthetic fibers by PKS extracts

The dyeability of natural (wool, cotton, ramie) and synthetic (acrylic, polyester,

nylon) fabrics by PKS extracts was examined to investigate the potential dyeability of the

extracts. Synthetic fibers (especially polyester and polyacrylonitrile) are generally dyed

Chapter 3

only by disperse dyestuffs and it is expected that polyester and polyacrylonitrile are not dyed by PKS extracts. However, acrylic fiber having carboxylic groups is dyed by basic dyestuff and nylon is dyed by acid dyestuff. Therefore, it is interesting to try to dye synthetic fiber fabrics with PKS extracts.

The results show that wool fabric is dyed brownish orange by PKS extracts. Its colour is similar to that of dyed silk fabric. The cotton and ramie fabrics are dyed pale brown and brown. The dyeability of cotton is slightly low. On the other hand, acrylic and polyester fabrics are not dyed at all. However, nylon is dyed brownish orange. The measured colors for the natural and synthetic fiber fabrics by using PKS extracts are summarized in Table 3.5. As seen in Table 3.5, wool, cotton, ramie and nylon show lower L^* value and wool and nylon show higher a^* and b^* values. The results show that PKS extracts dye not only silk but also wool, cotton, ramie, and nylon under the dyeing condition used. It has important meaning from industrial point of view that nylon as synthetic fiber can be dyed by PKS extracts, because a variety of applications is expected to be developed.

Table 3.5. *L**, *a**, and *b** values obtained for wool, cotton, ramie, acrylic, polyester, and nylon fabrics.

Sample	Wool		Cotton		Ramie	
Dyed	Before	After	Before	After	Before	After
L*	87.6	55.0	94.8	61.0	93.1	52.7
a*	-0.180	20.2	-0.120	9.80	-0.110	12.0
b*	13.5	33.9	1.44	18.9	2.18	26.2

Sample	Acrylic		Polyester		Nylon	
Dyed	Before	After	Before	After	Before	After
L*	94.1	89.2	94.2	94.8	94.6	57.4
a*	-1.36	1.09	-0.448	0.0284	-1.02	17.1
b*	8.67	1.31	1.87	4.47	9.16	44.5

Before and after dyed with $x_f = 0.010$ at 60°C for 180 min.

Silk, wool and ramie are dyed deeper than cotton and nylon under same dyeing conditions. Silk and wool have many kinds of hydrophilic functional groups, including ionisable groups and nylon contains actually a few amounts of ionisable groups. On the other hand, ccotton and ramie have hydroxyl groups. The results show that the dyestuffs in PKS extracts show affinity to fiber materials which have hydrophilicity. It can be said that silk and wool are proteins having hydrophilic functional groups and they are favourable to dyeing with the water-soluble dyestuffs in PKS extracts. The chemical and physical structure of ramie may be suited for the dyeing with the dyestuffs. The dyeability

of fibre materials depends upon not only interactions between network frame molecules/functional groups and dye molecules, but also higher ordered structures of matrices in fibres, which control the penetration and diffusion of dye molecules, as is known. The many complicated factors result in the dyeability for each of the fibres. Furthermore, it is also thought that dye-producing reaction (oxidation and coupling reactions) could proceed both at inside and outside of fibers. The dyeing process should be very complicated. While it is very difficult, further study is needed to clarify the dyeing mechanism.

3.4. Conclusion

Silk, wool, cotton, ramie and nylon fibers can be dyed by water-extracts from palm kernel shell of oil palm tree. The dyeability for silk fabric by the palm kernel shell extracts increases with increasing dyeing time and temperature. The dyeability for silk fabric by the palm kernel shell extracts with an increase in the amount of extracts in the dyeing solution shows interesting behaviour that hue changes and the lightness decrease and slightly increases with an increase in the supplied amount of extracts. The colourants in the palm kernel shell extracts is thought to be oxidised during dyeing process. Such chemical change of the colourants and the formation of dye molecules aggregation may influence the dyeing behavior.

Chapter 3

References

[1] United States Department of Agriculture, Foreign Agricultural Service, *Production, Supply and Distribution (PSD) Database*, *Palm Oil*: *World Supply and Distribution* (2019)

[2] Awalludin, M. F., Sulaiman, O., Hashim R., and Nadhari, W. N. A. W.; An overview of the oil palm industry in Malaysia and its waste utilization through thermochemical conversion, specifically via liquefaction, *Renewable and Sustainable Energy Reviews*, 50, 1469–1484 (2015)

[3] Nguyễn, T. K. T., Kuroda, A., Urakawa, H., and Yasunaga, H.; Dyeing fabrics by using extracts from mulberry branch/trunk 1. Dyeability and fluorescence property, *American Journal of Plant Sciences*, 8, 1888–1903 (2017)

[4] Ozen, E., Yeniocak, M., Colak, M., Goktas, O., and Koca, İ.; Colorability of wood material with *Punica granatum* and *Morus nigra* extracts, *BioResources*, 9, 2797–2807 (2014)

[5] Robertson, A. R.; Color-Difference Formulae, *Color Research* and *Application*, 2, 7–11 (1977)

[6] Commission Internationale de l′Eclairage, *Colorimetry* – Part 4: CIE 1976 $L*a*b*$ Colour space, CIE S 014-4/E:2007 (ISO 11664-4:2008(E)), Switzerland (2007)

[7] Kubelka, P. and Munk, F.; Ein beitrag zur optik der farbanstriche, *Zeitschrift für Technische Physik*, 12, 593–601 (1931)

[8] Kubelka, P.; New Contributions to the optics of intensely light-scattering materials. Part I, *Journal of the Optical Society of America*, 38, 448–457 (1948)

[9] Tsouko, E., Alexandri, M., Fernandes, K. V., Freire, D. M. G., Mallouchos A., and Koutinas, A. A.; Extraction of phenolic compounds from palm oil processing

residues and their application as antioxidants, *Food Technology and Biotechnology*, 57, 29–38 (2019)

[10] Yasunaga, H., Takahashi, A., Ito, K., Ueda M., and Urakawa H.; Hair dyeing by using catechinone obtained from (+)-catechin, *Journal of Cosmetics, Dermatological Sciences and Applications*, 2, 158–163 (2012)

[11] Matsubara, T., Seki C., and Yasunaga, H.; Relationships between Sspecies of dyestuff precursor and dyeability in hair colouring made by enzymatic oxidation technique using bio-catechols, *American Journal of Plant Sciences*, 8, 1471–1483 (2017)

[12] Corbett, J. F.; Chemistry of hair colorant processes. Science as an aid to formulation and development, *Journal of the Society of Cosmetic Chemists of Japan*, 35, 297–310 (1984)

[13] Vickerstaff, T.; *The Physical Chemistry of Dyeing*, Chapter V, Oliver and Boyd, London (1954)

[14] Matsubara, T., Wataoka, I., Urakawa, H., and Yasunaga, H.; Effect of reaction pH and $CuSO_4$ addition on the formation of catechinone due to oxidation of (+)-catechin, *International Journal of Cosmetic Science*, 35, 362–367 (2013)

[15] Neo, Y. P., Ariffin, A., Tan C. P., and Tan, Y. A.; Determination of oil palm fruit phenolic compounds and their antioxidant activities using spectrophotometric methods, *International Journal of Food Science and Technology*, 43, 1832–1837 (2008)

[16] Ahamad, N., Hassan, Z. A. A., Muhamad, H., Bilal, S. H., Yusof, N. Z., and Idris, Z.; Determination of total phenol, flavonoid, antioxidant activity of oil palm leaves extracts and their application in transparent soap, *Journal of Oil Palm Research*, 30, 315–325 (2018)

Chapter 3

[17] Vickerstaff, T.; *The Physical Chemistry of Dyeing*, Chapter III, Oliver and Boyd, London (1954)

[18] Guyot, S., Vercauteren J., and Cheynier, V.; Structural determination of colourless and yellow dimers resulting from (+)-catechin coupling catalysed by grape polyphenoloxidase, *Phytochemistry*, 42, 1279–1288 (1996)

[19] Brown, A. G., Falshaw, C. P., Haslam, E., Holmes, A. and D. Ollis, W.; The constitution of theaflavin, *Tetrahedron Letters*, 7, 1193–1204 (1966)

[20] Tanaka, T. and Kouno, I.; Oxidation of tea catechins: Chemical structures and reaction mechanism, *Food Science and Technology Research*, 9, 128–133 (2003)

Chapter 4

General Conclusion

The purpose of this study is producing cellulose nanofiber and dye from oil palm tree. This thesis consists of four chapters, the essence of each chapter is as follows.

In Chapter 1, it was reported on background of this thesis and present state regarding the production of cellulose nanofiber and natural dyes. Especially these materials were over viewed in historic and global point of view and summarized and the purpose of this study was described.

In Chapter 2, cellulose nanofibers (CNFs) were obtained from three types of oil palm wastes, palm pressed fiber (PPF), empty fruit bunch (EFB), and palm kernel shell (PKS), as well as the trunk of the oil palm tree, to compare their morphological, thermal, and mechanical properties. Despite large differences in the chemical components of cell walls in the raw materials, the production of CNFs from all parts of the oil palm were achieved in this work. The morphology and mechanical properties of the CNF sheets obtained from the trunk had advantages over the CNF sheets from wastes, while the thermal degradation properties showed no advantage. Cellulose crystallinity of the CNF sheet from the PPF and PKS had lower crystallinity (69.1 and 71.1%), and the highest crystallinity of 77.0% was exhibited by the sheet from the trunk. The value of specific tensile strength and specific Young's modulus were highest in the CNF sheet of the trunk, and lowest mechanical properties shown in the CNF sheet from the PPF. These results strongly suggested that the CNF could be obtained from all parts of the plants, but their properties may vary.

Chapter 4

In Chapter 3, the dyeing of fabrics by using the extracts from trunk, empty fruit bunch, PPF and palm kernel shell (PKS) of oil palm trees was tried and the relationships between dyeing conditions and dyeability were studied. It was found that the PKS extracts obtained by the extraction with water dye silk fabric brownish orange color and they show highest dyeability among the extracts. The dyeing results for silk fabric by PKS extracts with an increase in the amount of extracts in the dyeing solution do not show general dyeing behaviour. The hue of dyed silk changes and the lightness decreases and then slightly increases with an increase in the supplied amount of extracts. It indicates that the colourants in PKS extracts may be oxidised and they change chemically during dyeing process and/or the colourant molecules might form aggregates and the composition of dyestuffs adsorbed on fibre varies. The dyeability of silk by PKS extracts increases with increasing dyeing time and temperature. Furthermore, it was revealed that wool, cotton, ramie and nylon are also dyed by PKS extracts. This study has clarified for the first time that the extracts from PKS of oil palm trees work as a useful dye dyestuff.

These achievements of this study are considered to be superior in promoting effective utilization of oil palm waste and producing hopeful material of cellulose nanofiber and interesting natural dye. In the future, it is expected to environmentally benign materials contribute to keep global environment and economics of Japan and Thailand.

Publication List

1. Yoko Okahisa, Yuma Furukawa, Kiyoaki Ishimoto, Chieko Narita, Kamthorn Intharapichai, Hitomi Ohara, Comparison of cellulose nanofiber properties produced from different parts of the oil palm tree, *Carbohydrate Polymers*, 198, 313–319 (2018)

2. Kamthorn Intharapichai, Akari Oda, Yoko Okahisa, Hitomi Ohara, and Hidekazu Yasunaga, Relationships between Dyeing Conditions and Dyeability of Extracts from Oil Palm Tree, *Journal of Fiber Science and Technology*, 76, 95–103 (2020)

Acknowledgements

The author really indebted to Ms. Kaori Oda at Department of Biobased Materials Science, Kyoto Institute of Technology for kindness, assistance and everyday help in work.

Finally, the author expresses his deep appreciation to his family members for constant encouragement and understanding during his research life.